

Articles

Contribution from the Department of Chemistry,
Wayne State University, Detroit, Michigan 48202

Synthesis, Spectroscopy, and Photophysical Behavior of Mixed-Ligand Mono- and Bis(polypyridyl)chromium(III) Complexes. Examples of Efficient, Thermally Activated Excited-State Relaxation without Back Intersystem Crossing¹

Chong Kul Ryu and John F. Endicott*

Received September 3, 1987

A series of $\text{Cr}^{\text{III}}(\text{PP})_n\text{X}_{6-2n}$ complexes have been prepared and characterized in which $n = 1$ or 2 , $\text{PP} = 2,2'$ -bipyridine or $1,10$ -phenanthroline, and $\text{X} = \text{NH}_3$, $\text{en}/2$, $\text{acac}^-/2$, CN^- , or NCS^- . The $(^2\text{E})\text{Cr}^{\text{III}}(\text{PP})_n\text{X}_{6-2n}$ excited states are much weaker oxidants than their $(^2\text{E})\text{Cr}(\text{PP})_3^{2+}$ parents. The visible spectroscopy of the $\text{Cr}^{\text{III}}(\text{PP})_n\text{X}_{6-2n}$ complexes is complicated by overlapping absorptions. A very prominent feature of these absorptions is a regular, relatively narrow band progression with energies independent of X . This progression is attributed to direct excitation into the triplet- π^* ligand manifold of states, with the forbidden singlet-triplet transitions of the free polypyridyl ligand(s) being relaxed by spin-spin coupling in the $\text{Cr}(\text{III})$ complexes. The $(^2\text{E})\text{Cr}(\text{III})$ lifetimes, $\tau(^2\text{E})$, of these complexes in fluid and glassy solutions are strongly temperature dependent but approach a limiting value at low temperatures: $[\tau(^2\text{E})]^{-1} = k_r + k_{nr}^0 + A \exp(-E_a/RT)$, where k_r and k_{nr}^0 are the nearly temperature-independent radiative and nonradiative relaxation rate constants, respectively. The room-temperature lifetimes (in $\text{DMSO} + \text{H}_2\text{O}$ solution) of the mixed-ligand complexes vary over a 30-fold range, and $\tau(^2\text{E})$ is much smaller for these complexes than found for their $\text{Cr}(\text{phen})_3^{3+}$ and $\text{Cr}(\text{bpy})_3^{3+}$ parents. The range of lifetimes is not strongly temperature dependent since $E_a = 33 \pm 2 \text{ kJ mol}^{-1}$ and $A = (3.5 \pm 1.1) \times 10^{11} \text{ s}^{-1}$ for the $\text{Cr}^{\text{III}}(\text{PP})_n\text{X}_{6-2n}$ complexes ($\text{X} \neq \text{CN}^-$); for $\text{X} = \text{CN}^-$, $A \sim 7 \times 10^{12} \text{ s}^{-1}$. All these complexes are characterized by large differences in energy between their lowest energy quartet and doublet excited states ($\Delta E > 64 \text{ kJ mol}^{-1}$). The most likely thermally activated relaxation channel in solution is inferred to involve nuclear rearrangements appropriate to a conventional surface crossing. The solvent must contribute significantly to this activation barrier.

Introduction

The excited-state behavior of chromium(III) has long challenged the imaginations of a variety of researchers.² For example, the energies of the lowest $\text{Cr}(\text{III})$ excited states often exceed the energy requirements of more than one ground-state substitutional process, yet the photoinduced substitutions are reasonably selective and usually antithermal. Regularities in the photosubstitutional behavior have been summarized by Adamson³ in a simple set of "rules", and they have been the subject of theoretical analyses by Zink⁴ and by Vanquickenborne and Ceulemans.⁵ These theoretical approaches^{4,5} have been remarkably successful in predicting the ligand most likely to be labilized and in rationalizing the photoinduced stereochemical changes, even though they are based on orbital populations in Franck-Condon quartet excited states and a presumed photodissociative reaction pathway. These premises are of questionable validity since the photoproducts form after the excited molecule has relaxed to the lowest energy excited state of many $\text{Cr}(\text{III})$ complexes, and the observed pressure dependence of product yields and the excited-state lifetimes are more consistent with an associative than with a dissociative photoreaction pathway.^{2d,6,7}

The lowest energy doublet excited states $(^2\text{E})\text{Cr}(\text{III})$ are a unique class of electronic excited states in that their orbital populations and their molecular geometries are almost always identical with those of the ground state.² Despite this lack of excited-state distortion, the unimolecular processes quenching $(^2\text{E})\text{Cr}(\text{III})$ excited states often result in the efficient formation of products. This paradoxical situation has led to the hypothesis that the dominant $(^2\text{E})\text{Cr}(\text{III})$ electronic relaxation process involves back intersystem crossing (BISC) to thermally populate a distorted quartet excited state.^{2a-c} Alternative hypotheses have proposed that products are formed directly from $(^2\text{E})\text{Cr}(\text{III})$ ⁸ or that the $(^2\text{E})\text{Cr}(\text{III})$ relaxation involves an electronically "forbidden" surface crossing to an intermediate in its ground electronic state.⁹

The $(^2\text{E})\text{Cr}(\text{III})$ excited-state lifetimes vary over more than a millionfold range and depend strongly on the coordinated ligands, the condensed-phase medium, and the temperature.² $\text{Cr}(\text{bpy})_3^{3+}$ and $\text{Cr}(\text{phen})_3^{3+}$ complexes have ^2E excited states that are among the most long-lived in ambient aqueous solutions.^{2d,e} The relatively long lifetimes of these complexes have been ascribed to their relatively large quartet-doublet excited-state energy differences.^{2c,e}; thus, the photochemistry and the thermally activated $(^2\text{E})\text{Cr}(\text{PP})_3^{3+}$ excited-state relaxation are almost universally ascribed to doublet excited-state behavior.^{2e,10} In connection with this view, some arguments have been advanced for reaction and quenching by means of an associative reaction of $(^2\text{E})\text{Cr}(\text{PP})_3^{3+}$.^{2e} Alternatively, the large activation energy (about 42 kJ mol^{-1})¹¹ associated with the thermally activated, nonradiative relaxation of these complexes could be a measure of the excited-state quartet-doublet energy gap, $\Delta E = E(^4\text{T}_2^0) - E(^2\text{E}^0)$.

- (1) Partial support of this research by the National Science Foundation and the Department of Energy, Office of Basic Energy Sciences, is gratefully acknowledged.
- (2) For reviews see: (a) Balzani, V.; Carasitti, V. *Photochemistry of Coordination Compounds*; Academic: New York, 1970. (b) Zinato, E. In *Concepts of Inorganic Photochemistry*; Adamson, A. W., Ed.; Wiley: New York, 1975; Chapter 4. (c) Kirk, A. D. *Coord. Chem. Rev.* **1981**, *39*, 225. (d) Endicott, J. F.; Ramasami, T.; Tamarasani, R.; Lessard, R. B.; Ryu, C. K.; Burbaker, G. R. *Coord. Chem. Rev.* **1987**, *77*, 1. (e) Jamieson, M. A.; Serpone, N.; Hoffman, M. Z. *Coord. Chem. Rev.* **1981**, *39*, 121.
- (3) Adamson, A. W. *J. Phys. Chem.* **1967**, *71*, 798.
- (4) (a) Zink, J. J. *Am. Chem. Soc.* **1972**, *94*, 8039. (b) *Mol. Photochem.* **1973**, *5*, 151. (c) *Inorg. Chem.* **1973**, *12*, 1957. (d) *J. Am. Chem. Soc.* **1974**, *96*, 4464.
- (5) (a) Vanquickenborne, L. G.; Ceulemans, A. *Coord. Chem. Rev.* **1983**, *48*, 157. (b) *J. Am. Chem. Soc.* **1977**, *99*, 2208. (c) *J. Am. Chem. Soc.* **1978**, *100*, 475. (d) *Inorg. Chem.* **1979**, *18*, 3475. (e) *Inorg. Chem.* **1979**, *18*, 897.

- (6) Lee, S. H.; Waltz, W. L.; Demmer, D. R.; Walters, R. T. *Inorg. Chem.* **1985**, *24*, 1531.
- (7) Endicott, J. F.; Ryu, C. K. *Comments Inorg. Chem.* **1987**, *6*, 91.
- (8) Gutierrez, A. R.; Adamson, A. W. *J. Phys. Chem.* **1978**, *82*, 902.
- (9) Endicott, J. F.; Ferraudi, G. J. *J. Phys. Chem.* **1976**, *80*, 949.
- (10) (a) Rojas, G. E.; Magde, D. *J. Phys. Chem.* **1987**, *91*, 689. (b) Rojas, G. E.; Magde, D. *Inorg. Chem.* **1987**, *26*, 2335.
- (11) Allsopp, S. P.; Cox, A.; Kemp, T. J.; Reed, W. J.; Sostero, S.; Traverso, O. *J. Chem. Soc., Faraday Trans. 1* **1980**, *76*, 162.

We have prepared a series of $\text{Cr}^{\text{III}}(\text{PP})_n\text{X}_{6-2n}$ complexes (PP = bpy, phen; $n = 1, 2$; X = NH_3 , CN^- , NCS^- , en/2, $\text{acac}^-/2$) in order to examine the effect of systematic variations in the quartet and doublet excited-state energies on $(^2\text{E})\text{Cr}(\text{III})$ photophysical behavior. In this paper we describe the synthesis and characterization of these compounds, aspects of their absorption and emission spectroscopy, and the temperature dependence of their $(^2\text{E})\text{Cr}(\text{III})$ lifetimes in the range 77–298 K. The excited-state doublet–quartet energy gap varies through a range of approximately 64–113 kJ mol^{-1} for this series of compounds. Consequently, we have been able to use these compounds to investigate the relationship between their photophysical behavior and ΔE . Our observations are not consistent with the BISC hypothesis, at least in its simplest form.

Experimental Section

A. Syntheses. The preparations of *cis*- $\text{Cr}[(\text{phen})_2\text{Cl}_2]\text{Cl}\cdot 2\text{H}_2\text{O}$ and *cis*- $[\text{Cr}(\text{phen})_2(\text{H}_2\text{O})_2](\text{NO}_3)_3$ have been described elsewhere.^{12–14} 2,2'-Bipyridine (99%) and 1,10-phenanthroline monohydrate (99%) (Aldrich) were used without further purification. The reddish brown *cis*- $[\text{Cr}(\text{phen})_2\text{Cl}_2]\text{Cl}\cdot 2\text{H}_2\text{O}$ was dried at 80 °C until the color turned to green; the green *cis*- $[\text{Cr}(\text{bpy})_2\text{Cl}_2]\text{Cl}\cdot 2\text{H}_2\text{O}$ was dried overnight at 80 °C before using. All other chemicals were reagent grade or better and were used as received. The other mixed-ligand (polypyridyl)chromium(III) complexes were prepared as follows.

***cis*- $[\text{Cr}(\text{phen})_2(\text{NH}_3)_2](\text{ClO}_4)_3\cdot \text{H}_2\text{O}$.** This complex was prepared according to the reported method¹⁵ except that the dry *cis*- $[\text{Cr}(\text{phen})_2\text{Cl}_2]\text{Cl}\cdot 2\text{H}_2\text{O}$ (3 g) was suspended and stirred in liquid ammonia (about 150 mL) that contained a trace of Na metal and ferric ammonium sulfate, $\text{Fe}(\text{NH}_4)(\text{SO}_4)_2$.¹⁶ This modified method yielded only the desired complex, which was purified by using the method in literature.¹⁵

$[\text{Cr}(\text{phen})_2(\text{acac})](\text{ClO}_4)_2$. A 0.5-g sample of *cis*- $[\text{Cr}(\text{phen})_2(\text{H}_2\text{O})_2](\text{NO}_3)_3\cdot 4\text{H}_2\text{O}$ was dissolved in 15 mL of DMF, and when necessary, the solution was filtered to remove any residues. The volume of the filtrate was reduced to about 10 mL by rotatory evaporation under reduced pressure. A stoichiometric amount of the distilled 2,4-pentanedione was added to the solution at room temperature. After being stirred for about 2 h, the solution was left overnight in the refrigerator. The light pinkish precipitate formed was filtered out, washed with ethanol and ether, and then air-dried. This compound was dissolved in a minimum amount of DMF and precipitated by an addition of LiClO_4 .

***cis*- $[\text{Cr}(\text{phen})_2(\text{TFMS})_2]\text{TFMS}$.** Nitrogen was bubbled through a solution of *cis*- $[\text{Cr}(\text{phen})_2\text{Cl}_2]\text{Cl}\cdot 2\text{H}_2\text{O}$ (5 g) in 20–30 mL of redistilled $\text{CF}_3\text{SO}_3\text{H}$ (TFMSH)¹⁷ at room temperature until the evolution of HCl gas had ceased (less than 1 day). The solution was then cooled in an ice–water bath, and ether was slowly added with vigorous stirring until the formation of the pink precipitate was complete. The precipitate was filtered out, washed several times with ether, and dried in a vacuum oven. This compound was used without further purification.

Warning! Perchlorate salts of Cr(III) are extremely hazardous.

***cis*- $[\text{Cr}(\text{phen})_2(\text{NCS})_2]\text{NCS}\cdot \text{H}_2\text{O}$.** A 3.3-g sample of *cis*- $[\text{Cr}(\text{phen})_2(\text{TFMS})_2]\text{TFMS}$ and 9 g of NaSCN (10-fold excess) were mixed in 100 mL of MeOH. With 10 min of refluxing, *cis*- $[\text{Cr}(\text{phen})_2(\text{TFMS})_2]\text{TFMS}$ dissolved and a deep orange precipitate started to form. The reflux was continued for $1/2$ h to complete the reaction. After the solution was cooled in an ice–water bath, the deep orange precipitate was filtered out, washed several times with cold water, cold EtOH, and ether, and then dried in a vacuum oven. The yield was quantitative. The crude product was dissolved in boiling MeOH and then precipitated by addition of NaSCN.

$[\text{Cr}(\text{phen})_2(\text{CN})_2][\text{Cr}(\text{phen})(\text{CN})_4]\cdot 2\text{H}_2\text{O}$. A 5-g sample of *cis*- $[\text{Cr}(\text{phen})_2\text{Cl}_2]\text{Cl}\cdot 2\text{H}_2\text{O}$ and 8.8 g of NaCN (10-fold excess) were dissolved with stirring in about 150 mL of water. The solution was slowly heated to 50 °C within 30 min, and that temperature was then maintained for 3–4 h, during which time a brown–yellow precipitate formed. Excess NaClO_4 was added to the solution after cooling in an ice–water bath, the

yellow precipitate was filtered out, washed several times with cold water, followed by acetone and ether, and finally air-dried (yield of the crude product was 3.3 g). This compound was purified by passing its solution through a lipophilic resin (LH-20-120, Sigma Chemical Co.) and eluting with MeOH/EtOH (3:1 v/v). The broad yellow band (second band) was collected and rotatory-evaporated under reduced pressure until almost dry. The yellow precipitate was dissolved in a minimum amount of MeOH, and this solution was diluted by adding half that volume of water. Upon standing several days at room temperature in the dark, the solution yielded yellow chunky crystals. These were filtered out, washed with cold water, followed by acetone and ether, and then dried in a vacuum oven. Several recrystallizations from MeOH and/or water with NaClO_4 yielded only a double salt, $[\text{Cr}(\text{phen})_2(\text{CN})_2][\text{Cr}(\text{phen})(\text{CN})_4]$.

$\text{Na}[\text{Cr}(\text{phen})(\text{CN})_4]\cdot 1.5\text{H}_2\text{O}$. A small quantity (milligram scale) of $\text{Na}[\text{Cr}(\text{phen})(\text{CN})_4]$ was isolated by passing a solution of the double salt $[\text{Cr}(\text{phen})_2(\text{CN})_2][\text{Cr}(\text{phen})(\text{CN})_4]$ through a cation resin (SP-C25-120, Sigma Chemical Co.) and eluting with 0.3 M NaCl very carefully. Most of the yellow compound deposited on the column during the separation due to the very poor solubilities of the double salt and probably $[\text{Cr}(\text{phen})_2(\text{CN})_2]\text{Cl}$ in water. The first yellow eluate was rotatory-evaporated to half its volume. Upon cooling in an ice water bath and the addition of NaClO_4 , a yellow precipitate immediately formed. It was dissolved in a minimum amount of MeOH, and then one-third volume of water containing a small amount of NaClO_4 was added. On standing several days at room temperature in the dark, the solution yielded yellow crystals, which were filtered out, washed with cold water, acetone, and ether, and finally dried in a vacuum oven.

Alternatively, a larger quantity of $\text{Na}[\text{Cr}(\text{phen})(\text{CN})_4]$ was carefully isolated from $[\text{Cr}(\text{phen})_2(\text{CN})_2][\text{Cr}(\text{phen})(\text{CN})_4]$ as follows. A 3-g sample of $[\text{Cr}(\text{phen})_2(\text{CN})_2][\text{Cr}(\text{phen})(\text{CN})_4]$ was dissolved in boiling MeOH. After all the precipitate dissolved, 3–4 g of NaClO_4 was added and the solution was boiled for 1.5–2 h. It was then diluted with an equal volume of water. The diluted solution was further heated at about 60 °C for 30 min and rotatory-evaporated under reduced pressure until formation of a yellow precipitate. The solution was cooled in an ice–water bath with stirring for about 30 min. The yellow precipitate obtained above (found to be the double salt) was filtered out and washed once with ice-cold water. The filtrate was further rotatory-evaporated until another yellow precipitate started to form. (**Caution!** The yellow precipitate formed in the early stages of the second rotatory evaporation should be filtered out and combined with the first yellow precipitate, i.e. double salt.) After addition of a small amount of NaClO_4 , the solution was cooled in an ice–water bath for 30 min, during which time most of the desired compound precipitated. It was filtered out, washed with cold water and acetone, followed by ether, and dried in a vacuum oven. This procedure was carefully monitored with FT-IR by looking at the region of the CN stretching frequencies and/or by examining luminescence spectra and lifetime measurements (see Results). When contaminated with the double salt, $\text{Na}[\text{Cr}(\text{phen})(\text{CN})_4]$ should be recrystallized or else the above procedure repeated.

$[\text{Cr}(\text{phen})(\text{en})_2](\text{ClO}_4)_3$. A 1.5-mL portion of ethylenediamine (99%) was added to 150 mL of ethanol that contained 5 g of *cis*- $[\text{Cr}(\text{phen})_2\text{Cl}_2]\text{Cl}\cdot 2\text{H}_2\text{O}$. While the mixture was refluxing, a yellow precipitate started to form within 30 min. The mixture was further refluxed for about 20 min. After the solution was cooled to room temperature, the yellow precipitate was filtered out, washed with MeOH and ether, and then air-dried (60% yield; small-scale preparations gave better yields). The recrystallization from water of this chloride salt was not successful. $[\text{Cr}(\text{phen})(\text{en})_2]\text{Cl}_3$ was dissolved in a minimum amount of water at 50 °C, and AgClO_4 was added until no more AgCl was precipitated. The AgCl precipitate formed was filtered and washed several times with water. An excess of NaClO_4 was added to the filtrate with stirring, and the solution was allowed to cool overnight in the refrigerator. The yellow precipitate was filtered out and washed several times with MeOH, followed by ether, and then dried in a vacuum oven. Without the AgClO_4 treatment, the elemental analyses always showed the mixed salts with a ratio $\text{ClO}_4^-:\text{Cl}^- \approx 0.6:0.4$. $[\text{Cr}(\text{phen})(\text{en})_2](\text{ClO}_4)_3$ is sparingly soluble in MeOH at room temperature.

***cis*- $[\text{Cr}(\text{bpy})_2(\text{CN})_2](\text{ClO}_4)_3$.** A 10-g sample of *cis*- $[\text{Cr}(\text{bpy})_2\text{Cl}_2]\text{Cl}\cdot 2\text{H}_2\text{O}$ was added with stirring to 150 mL of boiling water that contained 2.1 g of NaCN (10-fold excess). The reaction was stopped within 30 s by cooling the reddish brown solution in an ice–water bath, and excess NaClO_4 was then added. Upon cooling, a greenish yellow precipitate formed (sometimes brown–yellow). The brown impurity could be easily removed by treating with boiling MeOH. This method was reproducible. The greenish yellow precipitate was dissolved in a minimum amount of warm water (40–50 °C), and the residues were removed by filtration (mostly green impurity) with an ultrafine fritted glass filter. An adequate amount of NaClO_4 was added to the filtrate. Upon cooling in an ice–water bath, a yellow precipitate formed. It was filtered out, washed with

- (12) Burstall, F. H.; Nyholm, R. S. *J. Chem. Soc.* **1952**, 3570.
- (13) Inskeep, R. G.; Bjerrum, J. *Acta Chem. Scand.* **1961**, 15, 62.
- (14) Hancock, M. P.; Josephsen, J.; Schäffer, C. E. *Acta Chem. Scand., Ser. A* **1976**, A30, 79.
- (15) Josephsen, J.; Schäffer, C. E. *Acta Chem. Scand., Ser. A* **1977**, A31, 813.
- (16) *Inorganic Syntheses*; Audrieth, L. F., Ed.; McGraw-Hill: New York, 1950; Vol. III, p 153.
- (17) For details on handling $\text{CF}_3\text{SO}_3\text{H}$, see: (a) Dixon, N. E.; Jackson, W. G.; Lancaster, M. J.; Lawrence, G. A.; Sargeson, A. M. *Inorg. Chem.* **1981**, 20, 470. (b) *Inorganic Syntheses*; Shreeve, J. M., Ed.; Wiley: New York, 1986; Vol. 24, Chapter 5.

MeOH and ether, and then air-dried. The compound was recrystallized from a minimum amount of warm water containing NaClO₄. The final yield was about 5%.

Alternatively, *cis*-[Cr(bpy)₂(CN)₂](ClO₄) was obtained by mixing 5 g of *cis*-[Cr(bpy)₂Cl₂](Cl₂·2H₂O) and 9.6 g of NaCN (10-fold excess) in 100 mL of water. The mixture was maintained at 50 °C until all of the olive-drab precipitate dissolved (ca. 2–3 h). The reddish brown solution was subsequently treated as in the first method; the yield was about 10%, but this method is less reproducible than the first one.

cis-[Cr(bpy)₂(NCS)₂](SCN·0.5H₂O). *cis*-[Cr(bpy)₂(TFMS)₂](TFMS) was prepared the same way as *cis*-[Cr(phen)₂(TFMS)₂](TFMS). *cis*-[Cr(bpy)₂(NCS)₂](SCN) was prepared by a method similar to that used for *cis*-[Cr(phen)₂(NCS)₂](SCN) in MeOH solvent. *cis*-[Cr(bpy)₂(NCS)₂](SCN) was alternatively prepared as follows. A 3-g sample of *cis*-[Cr(bpy)₂(TFMS)₂](TFMS) was added with stirring to 100 mL of water at 80 °C that contained 9 g of NaSCN (10-fold excess). The solution turned orange within 1 h. Upon cooling in an ice-water bath, an orange precipitate formed. The orange precipitate was filtered out, washed several times with cold water and cold *i*-PrOH, followed by ether, and air-dried. The compound was dissolved in boiling MeOH and then precipitated by adding NaSCN. The yields for both methods were quantitative.

[Cr(bpy)(en)₂](ClO₄)₃. A 3-mL portion of ethylenediamine was added at 60 °C with stirring to a 40-mL solution of DMSO containing 5 g of *cis*-[Cr(bpy)₂Cl₂](Cl₂·2H₂O). A yellow precipitate formed within 2–3 min. The mixture was cooled in an ice-water bath, 30 mL of EtOH solution saturated with LiCl was added with stirring, and the yellow precipitate thus obtained was filtered out, washed with EtOH and ether, and then air-dried (>90% yield). Recrystallization of this chloride salt from water was not successful. The perchlorate salt was obtained by a similar method to that used for [Cr(phen)(en)₂](ClO₄)₃.

B. Spectroscopic Measurements. Solution absorption spectra were obtained with a Cary Model 14 recording spectrophotometer at ambient temperature. Infrared spectra were recorded on a Nicolet 20 DX FT-IR spectrometer employing KBr disks.

C. Elemental Analyses. These were done by the Central Instrumentation Facility (CIF), Department of Chemistry, Wayne State University, and/or by Midwest Microlab (Indianapolis, IN).

D. Electrochemistry. Cyclic voltammograms of each chromium(III) complex (1 mM in DMF) were run on a PAR 179 digital coulometer with a PAR 175 programmer using a sodium saturated calomel electrode (SSCE) as a reference, a platinum wire for the auxiliary electrode, and a Pt electrode and/or a hanging-mercury-drop electrode (HMDE) as the working electrode. The medium used was 0.1 M NaTFMS in DMF solvent unless otherwise specified. The solution was deaerated with ultrahigh-purity nitrogen gas passed through two chromous perchlorate-perchloric acid scrubbers, a CaSO₄ drying column, and a stabilizer (containing DMF). The reference electrode was separated from the sample chamber by two salt bridges. The bridge adjacent to the reference electrode contained a 0.13 M TEAP aqueous solution, and the one adjacent to the sample chamber contained the same medium used for the sample. Data collection and output for scan rates greater than 50 mV/s were accomplished with a Nicolet Model 2090-3C digital oscilloscope with pen output, disk record, and binary digital I/O.

E. Luminescence Spectra and Lifetime Measurements. The luminescence spectra were detected at right angles to the excitation beam. A Moletron UV-1000 nitrogen laser, which pumped to a DL-14 tunable dye laser, was used as the excitation source, and a Princeton Applied Research OMA-1 with SIT Vidicon was used as a detector. A Zenith 158 computer was used to control the triggering of the laser (gated to the vidicon sweep) and receive, correct, and store the spectra. Corrections for detector distortion were based on the atomic emission lines from a Philips Ne-arc lamp. The computer interfacing and customized software were developed by On Line Instrument Services, Inc., Jefferson, GA.

Samples were placed in 1-cm cuvettes contained in a PRA thermostated cell housing, which can be controlled for the temperature range from +80 to -120 °C with the use of a regulated circulating bath and/or a stream of cooled nitrogen gas passed through the liquid-nitrogen Dewar bottle. For the 77 K glass spectra and solid-sample spectra, a cylindrical fluorescence cell (5-mm o.d., clear fused-quartz Suprasil grade) was mounted into an EPR quartz (Suprasil) nitrogen Dewar flask (Wilmad Model WG-850 Q).

Emission spectra at ambient and low temperatures were obtained in the binary solvent DMSO/H₂O (1:1 v/v) unless otherwise specified. A potassium chromate solution was used as a filter for scattered light with λ_{ex} < 500 nm, and a brown glass cutoff filter (Kodak 3-67), for λ_{ex} = 500–536 nm. Deaerations were, if necessary, accomplished by nitrogen or argon gas passed through two chromous chloride solution scrubbers.

The lifetime measurements were accomplished with a movable mirror (45°) inserted between sample and OMA so as to be easily interchang-

Table I. Summary of Elemental Analyses of Cr^{III}(PP)_nX_{6-2n} Complexes

complex	% theory (found)			
	C	H	N	C/N
<i>cis</i> -[Cr(phen) ₂ (NH ₃) ₂](ClO ₄) ₃ ·H ₂ O·0.5NaClO ₄	34.98 (35.05)	2.94 (2.92)	10.20 (10.42)	3.43 (3.36)
[Cr(phen) ₂ (acac)](ClO ₄) ₂	48.96 (48.85)	3.40 (3.26)	7.88 (7.79)	6.21 (6.27)
<i>cis</i> -[Cr(phen) ₂ (NCS) ₂](SCN)	55.28 (55.59)	2.75 (2.59)	16.71 (17.06)	3.31 (3.26)
[Cr(phen)(CN) ₄][Cr(phen) ₂ (CN) ₂ ·2H ₂ O]	60.28 (60.00)	3.37 (3.15)	20.08 (20.12)	3.00 (2.98)
Na[Cr(phen)(CN) ₄ ·1.5H ₂ O]	49.75 (49.32)	2.87 (2.55)	21.76 (21.62)	2.29 (2.28)
[Cr(phen)(en) ₂](ClO ₄) ₃	29.35 (30.31)	3.72 (3.85)	12.91 (13.06)	2.29 (2.32)
<i>cis</i> -[Cr(bpy) ₂ (CN) ₂](ClO ₄)	51.22 (51.56)	3.10 (3.10)	16.29 (16.66)	3.14 (3.09)
<i>cis</i> -[Cr(bpy) ₂ (NCS) ₂](SCN)·0.5H ₂ O	50.45 (50.32)	3.13 (3.22)	17.90 (17.76)	2.82 (2.83)
[Cr(bpy)(en) ₂](ClO ₄) ₃	26.83 (27.19)	3.86 (3.93)	13.41 (13.71)	2.00 (1.98)

Table II. Characteristic Infrared Spectral Bands and Assignments of Cr^{III}(PP)_nX_{6-2n} Complexes

complex	obsd bands, cm ⁻¹	assignt
Cr(phen) ₂ (NH ₃) ₂ ³⁺	1640	δ _a (NH ₂) and ν(C=N)
	1340	δ _s (NH ₂)
	770	ρ _r (NH ₃)
Cr(phen) ₂ (acac) ²⁺	1550	ν(CO)
	1350	δ _s (CH ₃)
Cr(phen)(en) ₂ ³⁺	1590	δ _s (NH ₂)
	1140	ν(C=N)
	1050	ν(C=C)
	770	ρ _r (NH ₂)
	770	ρ _r (NH ₂)
Cr(phen)(CN) ₄ ⁻	2136 vw, 2143 vw	ν(CN)
[Cr(phen)(CN) ₄][Cr(phen)(CN) ₂]	2126 vw, 2141 vw	ν(CN)
Cr(phen) ₂ (NCS) ₂ ⁺	2060 vs	ν(CN)
Cr(bpy)(en) ₂ ³⁺	1595	δ _s (NH ₂)
	1140	δ(C—N)
	1045	δ(C—C)
	745	ρ _r (NH ₂)
	745	ρ _r (NH ₂)
Cr(bpy) ₂ (CN) ₂ ⁺	2133 vw	ν(CN)
Cr(bpy) ₂ (NCS) ₂ ⁺	2060 vs	ν(CN)

able between the two kinds of experiments (spectra and lifetime). Luminescence lifetimes were determined with a PRA 1551 photomultiplier detection system coupled to a Gould 4500 digital oscilloscope. In a typical experiment, 64–256 signals were accumulated and averaged. All other experimental conditions for lifetime measurements were the same as those for luminescence spectra.

Results

A. Preparations and Characterizations of Cr^{III}(PP)_nX_{6-2n} Complexes. A series of Cr^{III}(PP)_nX_{6-2n} complexes have been synthesized by metathesis of Cr(PP)₂Cl₂⁺ or Cr(PP)₂(TFMS)₂⁺ complexes with X (NH₃, CN⁻, NCS⁻, en/2, acac⁻/2) in good yield except for the Cr^{III}(PP)_n(CN)_{6-2n} complexes. But attempts to make Cr(PP)₂(en)₂³⁺ complexes have failed even if different starting materials Cr(PP)₂X₂⁺⁺ (X = Cl⁻, TFMS⁻, n = 1+; X = H₂O, n = 3+) reacted with various ratios of ethylenediamine under various conditions. The results of the elemental analyses are summarized in Table I.

The characteristic infrared spectral bands for the mixed (polypyridyl)chromium(III) complexes are given in the Table II. The infrared spectra of *cis*-Cr(PP)₂(NCS)₂⁺ complexes exhibit the CN stretching frequency at 2060 cm⁻¹, implying N-bonded complexes.¹⁸ The cyanide CN stretch of *cis*-Cr(bpy)₂(CN)₂⁺ complexes appears at 2133 cm⁻¹ as a very weak singlet. The cyanide CN stretches of the Cr(phen)(CN)₄⁻ and of the double salt

(18) Nakamoto, K. *Infrared and Raman Spectra of Inorganic and Coordination Compounds*, 3rd ed.; Wiley: New York, 1978; p 270.

Table III. UV-Vis Absorption Spectra of $\text{Cr}^{\text{III}}(\text{PP})_n\text{X}_{6-2n}$ and Related Complexes at 25 °C

complex	solvent	$10^{-3}\lambda_{\text{max}}, \text{cm}^{-1}$ ($\epsilon, \text{M}^{-1} \text{cm}^{-1}$)
$\text{Cr}(\text{NH}_3)_6^{3+}$ ^a	DMSO/glycerol (1:1)	21.64 (44), 28.90 (37.2)
$\text{Cr}(\text{en})_3^{3+}$ ^a	DMSO/glycerol (1:1)	21.88 (85.9), 28.49 (69.9)
$\text{Cr}(\text{CN})_6^{3-}$ ^b	H_2O	26.79 (80), 32.57 (55)
$\text{Cr}(\text{phen})_3^{3+}$ ^c	H_2O	22.03 (324), 23.54 (602), 24.69 (870)
$\text{Cr}(\text{bpy})_3^{3+}$ ^{c,d}	H_2O	22.00 (260), 23.40 (610), 25.10 (900)
$[\text{Cr}(\text{phen})_2(\text{NH}_3)_2](\text{ClO}_4)_3$ ^e	H_2O	21.64, 23.64
$[\text{Cr}(\text{phen})(\text{en})_2](\text{ClO}_4)_3$	H_2O	21.98 (70), 23.53 (72), 28.89 (732)
$\text{Na}[\text{Cr}(\text{phen})(\text{CN})_4]$	DMSO	24.04 (sh, 82), 24.88 (sh, 87), 28.41 (1000), 37.31 (2.8×10^4)
$[\text{Cr}(\text{phen})_2(\text{NCS})_2]\text{SCN}$	DMSO	19.61 (132), 28.57 (sh, 1.1×10^4), 36.76 (4.1×10^4)
$[\text{Cr}(\text{phen})_2(\text{acac})]\text{ClO}_4$	DMSO	19.61 (36), 23.36 (4.5×10^4)
$[\text{Cr}(\text{phen})_2(\text{CN})_2][\text{Cr}(\text{phen})(\text{CN})_4]$	DMSO	25.00 (broad, 86)
$[\text{Cr}(\text{bpy})(\text{en})_2](\text{ClO}_4)_3$	H_2O	21.51 (sh, 78), 22.32 (104), 23.92 (124), 25.64 (163)
$[\text{Cr}(\text{bpy})_2(\text{CN})_2]\text{ClO}_4$	DMSO	22.22 (sh, 156), 23.81 (sh, 362), 25.32 (sh, 519), 32.26 (2.9×10^4)
$[\text{Cr}(\text{bpy})_2(\text{NCS})_2]\text{SCN}$	DMSO	19.80 (134), 29.24 (sh, 4.4×10^3), 32.26 (7.1×10^3)

^a Reference 57. ^b Reference 28. ^c Reference 20. ^d Reference 19. ^e Reference 15.

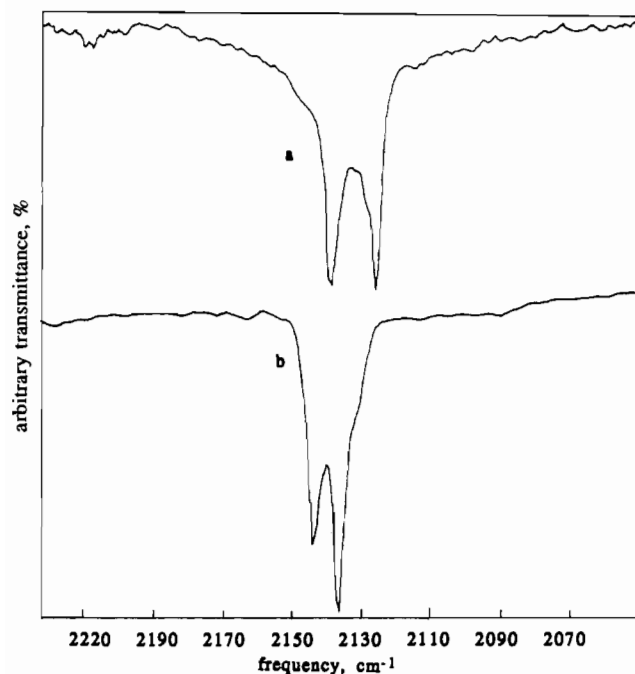


Figure 1. IR spectra at the region of the cyanide stretching frequencies: (a) $[\text{Cr}(\text{phen})_2(\text{CN})_2][\text{Cr}(\text{phen})(\text{CN})_4]$ at 2126 and 2141 cm^{-1} ; (b) $\text{Na}[\text{Cr}(\text{phen})(\text{CN})_4]$ at 2136 and 2143 cm^{-1} .

$[\text{Cr}(\text{phen})_2(\text{CN})_2][\text{Cr}(\text{phen})(\text{CN})_4]$ complexes appear as doublets at 2136 and 2143 cm^{-1} and at 2126 and 2141 cm^{-1} , respectively. While the doublet cyanide stretching bands for the double salt show more or less the same intensity, the lower energy band of the two cyanide stretching bands for $\text{Cr}(\text{phen})(\text{CN})_4^-$ is more intense than the higher energy band (Figure 1). This is valuable information when $\text{Cr}(\text{phen})(\text{CN})_4^-$ is isolated from the double salt, $[\text{Cr}(\text{phen})_2(\text{CN})_2][\text{Cr}(\text{phen})(\text{CN})_4]$. All cyanide stretching bands were extremely weak.

The rocking bands $\nu_r(\text{NH}_2)$ for $\text{Cr}(\text{phen})_2(\text{NH}_3)_2^{3+}$ and $\text{Cr}(\text{PP})(\text{en})_2^{3+}$ appear at somewhat higher energy than those for $\text{Cr}(\text{NH}_3)_6^{3+}$ (748 cm^{-1}) and $\text{Cr}(\text{en})_3^{3+}$ (720 cm^{-1}), respectively.¹⁸

The electronic absorption spectra for $\text{Cr}^{\text{III}}(\text{PP})_n\text{X}_{6-2n}$ complexes with their parent complexes are summarized in Table III, and the typical absorption spectra are shown in Figure 2. The absorption spectra of the mixed (polypyridyl)chromium(III) complexes are complicated by the strong ligand absorption in the ultraviolet region. All spectra except those for $\text{Cr}(\text{PP})_2(\text{NCS})_2^+$ complexes showed the two to four partly resolved bands that are similar to those observed in $\text{Cr}(\text{PP})_3^{3+}$ complexes^{19,20} except that their molar absorptivities, ϵ , are smaller than those in the parent $\text{Cr}(\text{PP})_3^{3+}$ complexes.

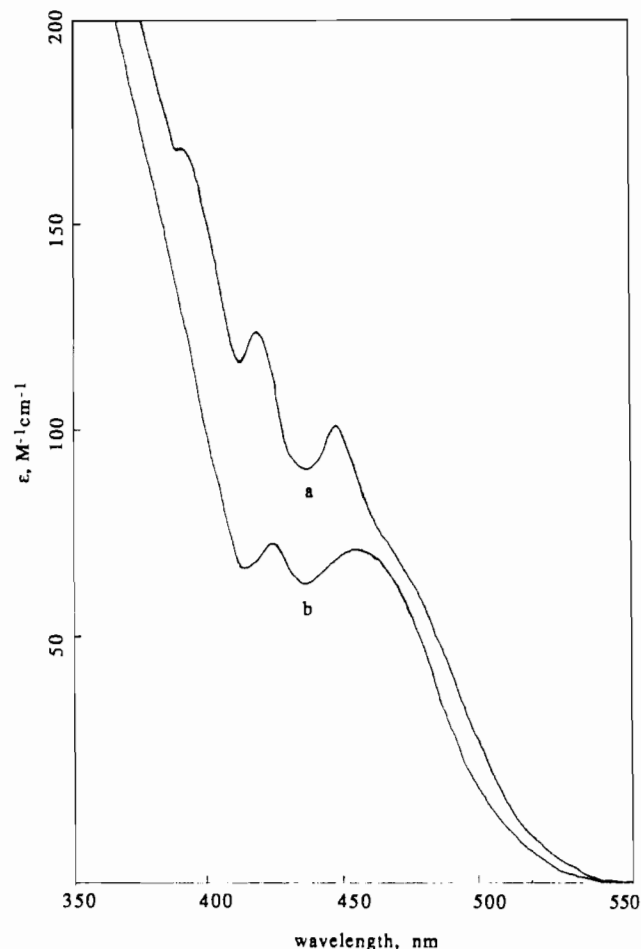


Figure 2. Typical electronic absorption spectra of $\text{Cr}(\text{PP})_n\text{S}_{6-2n}$ complexes in water at room temperature: (a) $\text{Cr}(\text{bpy})(\text{en})_2^{3+}$; (b) $\text{Cr}(\text{phen})(\text{en})_2^{3+}$.

Electrochemical data for $\text{Cr}^{\text{III}}(\text{PP})_n\text{X}_{6-2n}$ complexes are summarized in Table IV. Cyclic voltammograms of $\text{Cr}^{\text{III}}(\text{PP})_n\text{X}_{6-2n}$ in DMF in the potential range 0 to -1.6 V vs SSCE exhibit three reduction peaks for $n = 3$, two quasi-reversible and/or reversible reduction peaks ($\Delta E_p \sim 59$ mV)²¹ for $n = 2$ (Figure 3), and one reversible reduction peak for $n = 1$ (Figure 4). One quasi-reversible adsorption peak with 0.1 M NaTFMS in DMF always showed up at -0.26 ± 0.01 V vs SSCE with HMDE as a working electrode but not with the Pt electrode. Cyclic voltammograms of $\text{Cr}(\text{bpy})_3^{3+}$ and $\text{Cr}(\text{phen})_2(\text{NH}_3)_2^{3+}$ also exhibit one quasi-reversible reduction at about -1.3 V vs SSCE. However, this wave is not readily assigned. Cyclic voltammograms of $\text{Cr}(\text{PP})_2(\text{NCS})_2^+$ with 0.1 M NaTFMS in DMF each exhibit one ill-

(19) König, E.; Herzog, S. J. *J. Inorg. Nucl. Chem.* **1970**, *32*, 585.

(20) Serpone, N.; Jamieson, M. A.; Henry, M. S.; Hoffman, M. Z.; Bolleta, F.; Maestri, M. *J. Am. Chem. Soc.* **1979**, *101*, 2907.

(21) Nicholson, R. S.; Shain, I. *Anal. Chem.* **1964**, *36*, 706.

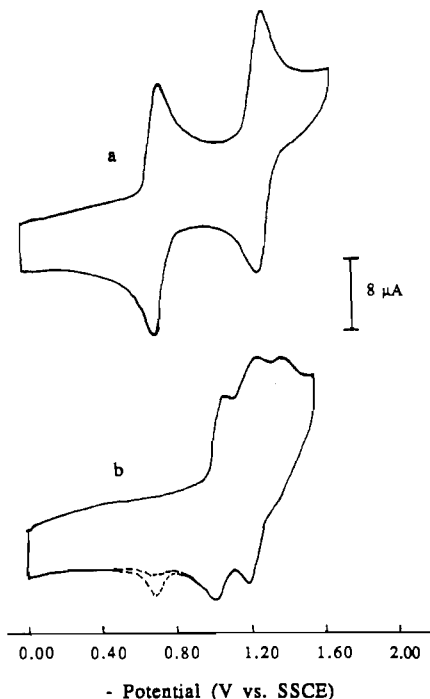


Figure 3. Cyclic voltammograms of 1 mM $\text{Cr}(\text{bpy})_2\text{X}_2^+$ in DMF at a platinum electrode (scan rate 1 V s^{-1} , room temperature): (a) $[\text{Cr}(\text{bpy})_2(\text{CN})_4]\text{ClJ}$ (0.1 M NaTFMS in DMF); (b) $[\text{Cr}(\text{bpy})_2(\text{NCS})_2]\cdot\text{SCN}$ (0.4 M NaSCN in DMF). The dotted line indicates the ill-defined peak (see text).

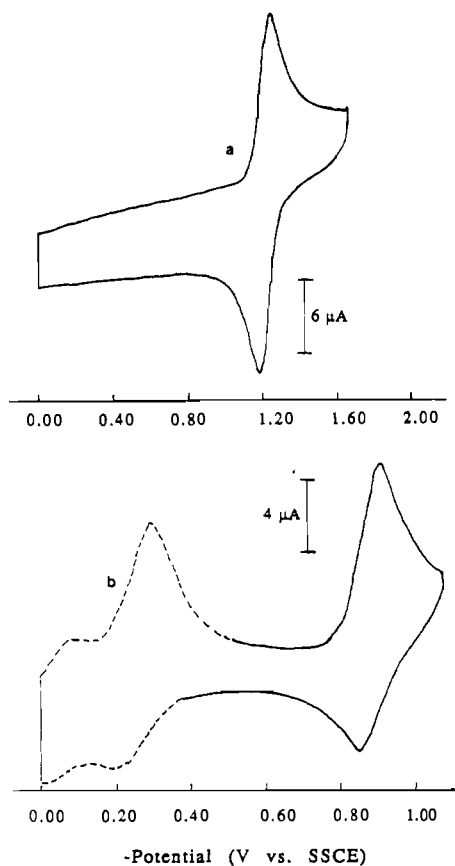


Figure 4. Cyclic voltammograms of 1 mM $\text{Cr}(\text{PP})\text{X}_4^+$ with 0.1 M NaTFMS in DMF (scan rate 1 V s^{-1} , room temperature): (a) $\text{Na}[\text{Cr}(\text{phen})(\text{CN})_4]$ (Pt electrode); (b) $[\text{Cr}(\text{bpy})(\text{en})_2](\text{ClO}_4)_3$ (HMDE electrode). The dotted line indicates the adsorption peak from DMF solvent.

defined oxidation peak at -0.68 ± 0.01 and $-0.71 \pm 0.02 \text{ V}$ vs SSCE for PP = phen and bpy, respectively. This wave was much smaller in 0.4 and 0.8 M NaSCN for $\text{Cr}(\text{bpy})_2(\text{NCS})_2^+$ and

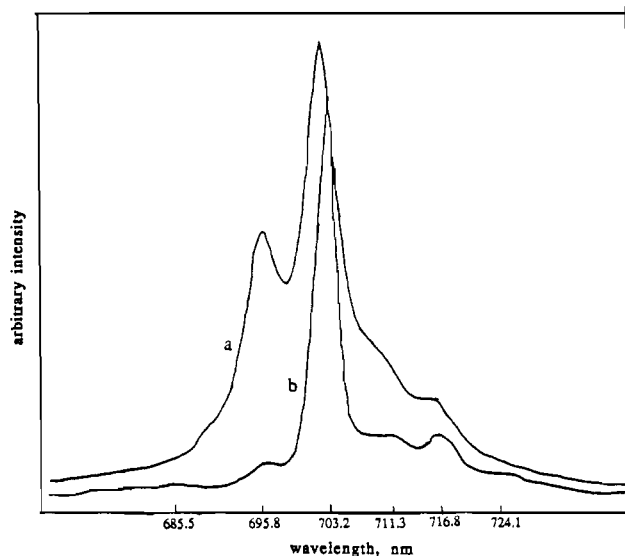


Figure 5. Doublet emission spectra of $\text{Cr}(\text{phen})_2(\text{NH}_3)_2^{3+}$ at (a) 222 K and (b) 77 K.

$\text{Cr}(\text{phen})_2(\text{NCS})_2^+$, respectively, in DMF, while the oxidation peaks at -1.00 ± 0.01 and $-0.99 \pm 0.01 \text{ V}$ vs SSCE increased in amplitude; the corresponding reduction peak was at $-1.07 \pm 0.02 \text{ V}$ vs SSCE for $\text{Cr}(\text{PP})_2(\text{NCS})_2^+$. This indicates that NCS^- substitutes rather rapidly during the electrochemistry. Cyclic voltammograms of $\text{Cr}^{\text{III}}(\text{PP})_n(\text{CN})_{6-2n}$ show two ($n = 2$; PP = bpy) and one ($n = 1$; PP = phen) reversible one-electron-transfer processes at $E_{1/2} = -0.737$ and -1.30 V vs SSCE for $n = 2$ and -1.225 V vs SSCE for $n = 1$, respectively. Cyclic voltammograms of $\text{Cr}(\text{PP})(\text{en})_2^{3+}$ were also consistent with a reversible one-electron-transfer process at $E_{1/2} = -0.890$ and -0.880 V vs SSCE for PP = phen and bpy, respectively.

Since the metal-centered, Cr(III)/Cr(II), reduction apparently overlapped with polypyridyl ligand reductions in several of the $\text{Cr}(\text{PP})_n\text{X}_{6-2n}$ complexes, we have also estimated potentials for these complexes in Table IV from the stoichiometrically weighted average of the Cr(III)/Cr(II) reduction potentials of the parent complexes.²² There is reasonable agreement between these estimates and the least negative value of $E_{1/2}$ for all except the NCS^- complexes. The $(^2\text{E})\text{Cr}^{\text{III}}(\text{PP})_n\text{X}_{6-2n}$ ($n < 3$) excited states are all weaker oxidants than are the $(^2\text{E})\text{Cr}(\text{PP})_3^{3+}$ parents.

B. Emission Spectra. The emission spectra of $\text{Cr}(\text{phen})_2(\text{NH}_3)_2^{3+}$, $\text{Cr}(\text{PP})(\text{en})_2^{3+}$, and $\text{Cr}(\text{bpy})_2(\text{CN})_2^+$ complexes show two different electronic origins in DMSO/ H_2O (1:1 v/v) at 77 K, similar to those observed in the parent $\text{Cr}(\text{PP})_3^{3+}$ complexes.²⁰ For noncentrosymmetric compounds, the most intense band in each spectrum is expected²³ to be the transition from the ^2E excited state to the ^4A ground state, and it is so assigned. The higher energy bands that we have observed are very weak at 77 K but become intense as temperature increases (Figure 5). This high energy, weak band cannot be a vibrational component of the ^2E band since there is no equivalent Stokes emission band. This higher energy band is tentatively assigned the transition from one of the upper $^2\text{T}_1$ components (see Discussion).

The details of the emission spectra are presented in Table V. The energy difference between the $^2\text{T}_1$ and ^2E excited states and the full width at half-maximum (fwhm) of the ^2E electronic origin were calculated and measured, respectively, on the basis of the emission spectra at 77 K.

The emission spectra of $\text{Cr}(\text{phen})(\text{CN})_4^-$ complexes show a somewhat broad (fwhm = 100 cm^{-1}), but intense single peak at 12748 cm^{-1} without any vibronic structure. The very weak emission spectrum of the double salt $[\text{Cr}(\text{phen})_2(\text{CN})_2][\text{Cr}$

(22) Niki, K.; Tanaka, N.; Yamada, A.; Itabashi, E.; Hartford, W. H. In *Encyclopedia of Electrochemistry of Elements*; Bard, A. J., Ed.; Dekker: New York, 1986; Vol. IX, Part B, Chapter IXb-4.

(23) Flint, C. D.; Greenough, P.; Matthews, A. P. *J. Chem. Soc., Faraday Trans. 2* 1973, 69, 419 and references therein.

Table IV. Reduction Properties of $\text{Cr}(\text{PP})_n\text{X}_{6-2n}$ and Their Parent Complexes^a

complex	tech- nique ^b	conditions	ΔE_p , mV ^c	$E_{1/2}$, V ^d	$-E_{1/2}$, V ^{d,e}	$10^{-3}E(^2E)$, cm ⁻¹ ^f	$E_{1/2}(*\text{Cr}^{3+}/\text{Cr}^{2+})$, V ^g
$\text{Cr}(\text{NH}_3)_6^{3+}$	P	0.01 M HCl + $(\text{NH}_4)_2\text{SO}_4$ ($\mu = 0.1$ M)	59	-0.880	0.88	15.23	1.01
		0.9 M KCl + 0.1 M acetate buffer		-1.0056			
$\text{Cr}(\text{NCS})_6^{3-}$	P	10 M KSCN	rev	-0.829	0.83	12.86	0.76
$\text{Cr}(\text{CN})_6^{3-}$	P	1 M KCN	60	-1.378	1.38	12.37	0.16
$\text{Cr}(\text{H}_2\text{O})_6^{3+}$				-0.65	0.65	14.75	1.18
CrCl_3	P	0.1 M TEAP in DMSO	60	-0.755	0.8		
			82	-0.915			
				-1.575			
$\text{Cr}(\text{en})_3^{3+}$	P	0.1 M acetate buffer		-0.855 to -0.875	0.86	14.96	1.0
		0.1 M KCl		-1.375			
$\text{Cr}(\text{acac})_3$	P	0.1 M TEAP in DMF	63	-1.723	1.7	12.8	~0.1
			49	-2.125			
$\text{Cr}(\text{bpy})_3^{3+}$	P	0.5 M NaCl	rev	-0.485	0.485	13.74	1.22
				-0.895			
				-1.275			
	CV	0.1 M NaTFMS in DMF ^h	61-78	-0.388			1.32
			65-80	-0.841			
			115-178	-1.193			
			82-111	(-1.358)			
$\text{Cr}(\text{phen})_3^{3+}$	P	0.1 M KCl	rev	-0.495	0.495	13.74	1.21
$\text{Cr}(\text{phen})_2(\text{NH}_3)_2^{3+}$	CV	0.1 M NaTFMS in DMF ⁱ	75-89	-0.888	0.6*-0.9	14.22	0.9-1.2
			75-88	-1.210			
$\text{Cr}(\text{phen})_2(\text{NCS})_2^+$	CV	0.8 M NaTFMS in DMF ^j	76-80	-1.022	(0.5*)-1.0	12.65	0.6
			72-82	-1.185			
$\text{Cr}(\text{phen})_2(\text{H}_2\text{O})_2^{3+}$	P	0.1 M KCl	rev	-0.735	0.6*-0.7		
			irr	-0.915			
			irr	-1.245			
$\text{Cr}(\text{phen})_2(\text{acac})_2^{2+}$	CV	0.1 M NaTFMS in DMF ^k	51-63	-0.727	0.7-0.8*		
			60-80	-1.200			
$\text{Cr}(\text{bpy})_2(\text{H}_2\text{O})_2^{3+}$	P	0.1 M KCl	rev	-0.715	0.6*-0.7		
			irr	-0.955			
			irr	-1.325			
$\text{Cr}(\text{bpy})_2\text{Cl}_2^+$	P	0.1 M KCl	rev	-0.725	0.6*-0.7		
			irr	-1.055			
			irr	-1.215			
$\text{Cr}(\text{bpy})_2(\text{NCS})_2^+$	CV	0.4 M NaSCN in DMF ^l	58-80	-1.017	(0.5*)-1.0	12.63	0.6
			82-86	-1.196			
$\text{Cr}(\text{bpy})_2(\text{CN})_2^+$	CV	0.1 M NaTFMS in DMF ^l	66-68	-0.739	0.7*	13.22	0.94
			65-70	-1.301			
$\text{Cr}(\text{phen})(\text{CN})_4^-$	CV	0.1 M NaTFMS in DMF ^l	65-70	-1.227	1.0*-1.2	12.75	0.38-0.58
$\text{Cr}(\text{phen})(\text{en})_2^{3+}$	CV	0.1 M NaTFMS in DMF ^m	65-73	-0.891	0.7*-1.9	14.36	0.88-1.08
$\text{Cr}(\text{bpy})(\text{en})_2^{3+}$	CV	0.1 M NaTFMS in DMF ^m	61-67	-0.876	0.7*-0.9	14.37	0.88-1.08

^aAll data for polarography from ref 22 and data for cyclic voltammetry from this work. ^bP stands for polarography and CV for cyclic voltammetry. ^cSlope (mV) for polarographic data. ^dV vs SSCE. ^eValues for Cr(III)/Cr(II) reduction potentials. Asterisks indicate values estimated by the stoichiometrically weighted average of the reduction potentials of their parent complexes. Values in parentheses are not consistent with observation. ^fLowest doublet excited-state energies. ^gReduction potentials of the lowest doublet excited-state energies (see text). ^hPt electrode; scan rate 0.2-1 V s⁻¹. ⁱHMDE; scan rate 0.2-1 V s⁻¹. ^jPt electrode; scan rate 0.05-1 V s⁻¹. ^kHMDE; scan rate 1-10 V s⁻¹. ^lPt electrode; scan rate 0.5-1 V s⁻¹. ^mHMDE; scan rate 1-5 V s⁻¹.

Table V. Emission Spectral Data for $\text{Cr}^{\text{III}}(\text{PP})_n\text{X}_{6-2n}$ in DMSO/H₂O (1:1 v/v) at 77 K

complex	$10^{-3}E(^2T_1)$, cm ⁻¹	$10^{-3}E(^2E)$, cm ⁻¹	ΔE , cm ⁻¹	fwhm(² E), cm ⁻¹
$\text{Cr}(\text{phen})_3^{3+}$ ^a	14.3	13.74	600	
$\text{Cr}(\text{phen})_2(\text{NH}_3)_2^{3+}$ ^b	14.37	14.22	150	60
$\text{Cr}(\text{phen})(\text{en})_2^{3+}$	14.57	14.36	210	90
$\text{Cr}(\text{phen})_2(\text{NCS})_2^+$		12.63		460 (280) ^c
$\text{Cr}(\text{phen})(\text{CN})_4^-$		12.75		110
$\text{Cr}(\text{bpy})_3^{3+}$ ^a	14.4	13.74	700	
$\text{Cr}(\text{bpy})(\text{en})_2^{3+}$	14.59	14.37	220	90
$\text{Cr}(\text{bpy})_2(\text{CN})_2^+$	13.49	13.22	270	59
$\text{Cr}(\text{bpy})_2(\text{NCS})_2^+$		12.65		334 (320) ^c

^aIn H₂O/MeOH (1:1 v/v) at pH 3.1; from ref 20. ^bReference 25. ^cIn DMF/CHCl₃ (3:1 v/v).

(phen)(CN)₄] at 77 K ($\lambda \approx 784$ nm) is indistinguishable from that observed in the $\text{Cr}(\text{phen})(\text{CN})_4^-$ complex, but the 77 K lifetime (~200 ns) is shorter.

The emission spectra of the $\text{Cr}(\text{PP})_2(\text{NCS})_2^+$ complexes are very broad and intense. The fwhm for $\text{Cr}(\text{phen})_2(\text{NCS})_2^+$ complexes depends on the medium used. For example, fwhm is 460 cm⁻¹ in DMSO/H₂O (1:1 v/v) at 77 K, but 28 cm⁻¹ in DMF/CHCl₃ (3:1 v/v) at 77 K. The spectral maximum is shifted but

not significantly (<2 nm). At 77 K the spectra of the $\text{Cr}(\text{phen})_2(\text{NCS})_2^+$ complex show a very weak impurity peak at 759.42 nm in DMSO/H₂O (1:1 v/v). This corresponds to emission from the $\text{Cr}(\text{phen})_2(\text{H}_2\text{O})_2^{3+}$ complex. We did not observe this impurity emission in DMF/CHCl₃ (3:1 v/v). On the basis of these observations and the ease of forming $\text{Cr}(\text{phen})_2(\text{H}_2\text{O})_2^{3+}$ during the synthesis in aqueous solution, it appears that the $\text{Cr}(\text{phen})_2(\text{NCS})_2^+$ complex aquates relatively rapidly. In contrast to the $\text{Cr}(\text{phen})_2(\text{NCS})_2^+$ complex, the spectral broadening and aquation under the same conditions for the $\text{Cr}(\text{bpy})_2(\text{NCS})_2^+$ complex were not important. The emission maxima of $\text{Cr}(\text{PP})_2(\text{NCS})_2^+$ complexes appear at lower energies than calculated from the average ligand field theory and even lower energy than $E(^2E)$ of the $\text{Cr}(\text{NCS})_6^{3-}$ complex (12.86×10^3 cm⁻¹).^{2d}

C. Excited-State Lifetime. To facilitate comparisons, most of the lifetimes were measured in the same binary solvent, DMSO/H₂O (1:1 v/v), between 77 and 298 K. More limited measurements were made in other solvent systems. The observed decays of the ²E excited states were fit to single exponentials in all temperature ranges for the complexes reported here.

The excited-state properties of the mixed (polypyridyl)chromium(III) complexes, $\text{Cr}^{\text{III}}(\text{PP})_n\text{X}_{6-2n}$, are summarized in Table VI. The mixed (polypyridyl)chromium(III) complexes, except for $\text{Cr}(\text{PP})_2(\text{NCS})_2^+$ complexes, have lifetimes comparable with

Table VI. Excited-State Properties of Cr^{III}(PP)_nX_{6-2n} and Related Complexes in DMSO/H₂O (1:1 v/v)

complex	10 ⁻³ E(⁴ T ₂ ⁰), cm ⁻¹	10 ⁻³ E(² E ⁰), cm ⁻¹	ΔE(⁴ T ₂ ⁰ - ² E ⁰), kJ mol ⁻¹	τ, μs		E _a , kJ mol ⁻¹	10 ⁻¹¹ A, s ⁻¹
				298 K	77 K		
Cr(NH ₃) ₆ ³⁺	19.96 ^b	15.23 ^c	56.6	2.2 ^b	78 ^d	38.0 ^d	11 ^d
Cr(en) ₃ ³⁺	20.18	14.96 ^c	62.4	1.85 ^d	100 ^d	41.0 ^d	120 ^d
Cr(CN) ₆ ³⁻	24.35	12.37	143.3	0.12 ^e	3950 ^e	30.5 ^f	1.4 ^f
Cr(NCS) ₆ ³⁻	16.42	12.86	42.6	~0.01 ^e	2380 ^e	39.2 ^f	347 ^f
Cr(phen) ₃ ³⁺	20.00	13.74 ^f	74.9	126 ^d	5300 ^e	38.0 ^d	0.6 ^d
Cr(bpy) ₃ ³⁺	20.00 ^h	13.74 ^f	74.9	73 ^e	5000 ^{g,i}	30.2 ^f	0.02 ^f
[Cr(phen)(en) ₂](ClO ₄) ₃	19.72	14.36	64.1	0.5	155	30.2	2.8
[Cr(bpy)(en) ₂](ClO ₄) ₃	19.75	14.37	64.4	0.5	164	29.5	2.4
Na[Cr(phen)(CN) ₄]	22.18	12.75	112.8	0.4	4320	32.8 ^j	57.7 ^j
						(20.7) ^k	(0.1) ^k
[Cr(phen) ₂ (NH ₃) ₂](ClO ₄) ₃ ^l	19.98	14.22 ^l	68.9	3.6 ^l	190 ^l	34.9 ^l	3.2 ^l
[Cr(bpy) ₂ (CN) ₂](ClO ₄) ₃	21.39	13.22	97.7	0.1	3600	33.6	100
[Cr(phen) ₂ (NCS) ₂](SCN)	18.21	12.63	66.8	2.2	660	34.8	5.1
					(820) ^m		
[Cr(bpy) ₂ (NCS) ₂](SCN)	18.21	12.65	66.5	2.8	610	34.8	4.1
					(750) ^m		

^a Calculated the lowest quartet excited-state energies, E(⁴T₂⁰), based on the origins of Cr(NH₃)₆³⁺ from ref 26 and Cr(bpy)₃³⁺ from ref 41; E(⁴T₂⁰)Cr(phen)₃³⁺ was assumed the same as that of Cr(bpy)₃³⁺; see text. ^b Reference 26. ^c Reference 57. ^d Reference 25 and references therein. ^e Reference 2d and references therein. ^f Reference 10, in MeOH + H₂O + glycol for Cr(CN)₆³⁻ and Cr(NCS)₆³⁻; H₂O + LiCl for Cr(bpy)₃³⁺. ^g Reference 20. ^h Reference 41. ⁱ Reference 64. ^j +25 to -28 °C. ^k -41 to -100 °C. ^l Reference 25. ^m In DMF/CHCl₃ (3:1 v/v).

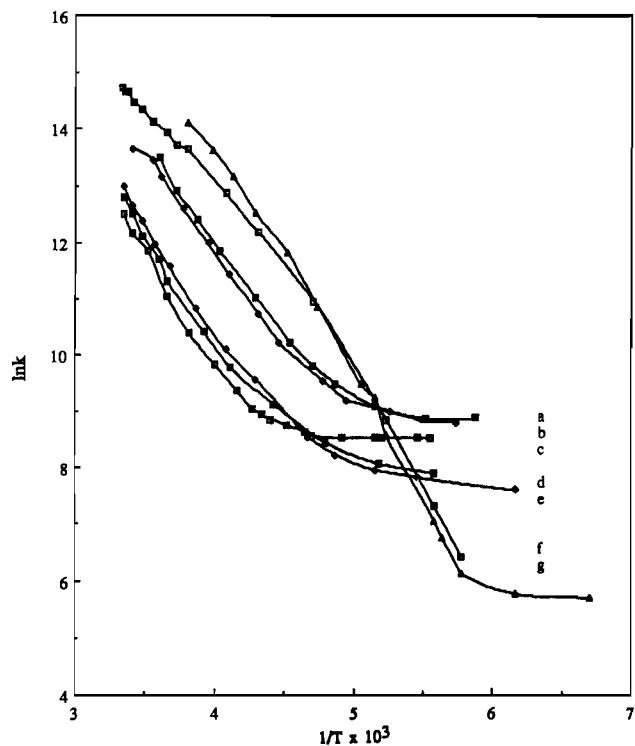


Figure 6. Thermally activated decays of (²E)Cr^{III}(PP)_nX_{6-2n} in DMSO/H₂O (1:0 v/v). Solid lines are used to connect experimental data for each compound: (a) Cr(bpy)(en)₂³⁺; (b) Cr(phen)(en)₂³⁺; (c) Cr(phen)₂(NH₃)₂³⁺; (d) Cr(bpy)₂(NCS)₂⁺; (e) Cr(phen)₂(NCS)₂⁺; (f) Cr(phen)(CN)₄⁻; (g) Cr(bpy)₂(CN)₂⁺.

those of their relatively short-lived, monodentate parent complexes at 298 and 77 K. The Cr(PP)₂(NCS)₂⁺ complexes have longer lifetimes at 298 K but shorter lifetimes at 77 K than does Cr(NCS)₆³⁻.

The observed temperature-dependent lifetime data for the mixed (polypyridyl)chromium(III) complexes could be fitted to an expression of the form shown in eq 1-3,^{2d,11,24} where k(TI) is the

$$k = [\tau(^2E)]^{-1} = k(\text{TI}) + k(T) \quad (1)$$

$$k(\text{TI}) = k_r + k_{nr}^0 \quad (2)$$

$$k(T) = A \exp(-E_a/RT) \quad (3)$$

(24) Endicott, J. F.; Tamilarasan, R.; Lessard, R. B. *Chem. Phys. Lett.* **1984**, *112*, 381.

Table VII. Ligand Field Parameters of Cr^{III}(PP)_nX_{6-2n} and Related Complexes

complex	10Dq ^a × 10 ⁻³ , cm ⁻¹	10 ⁻³ E(² E), cm ⁻¹	B ₅₅ ^b , cm ⁻¹	β ₅₅ ^c
Cr(NH ₃) ₆ ³⁺ ^d	21.64	15.23	878	0.96
Cr(en) ₃ ³⁺ ^d	21.88	14.96	856	0.93
Cr(CN) ₆ ³⁻ ^e	26.40	12.37	660	0.72
Cr(NCS) ₆ ³⁻ ^e	17.80	12.86	746	0.81
Cr(phen) ₃ ³⁺ ^f	23.36	13.74	761	0.83
Cr(bpy) ₃ ³⁺ ^{f,g}	23.24	13.74	761	0.83
cis-Cr(phen) ₂ (NH ₃) ₂ ³⁺	22.60	14.22	798	0.87
Cr(phen)(en) ₂ ³⁺	22.73	14.36	806	0.88
Cr(bpy)(en) ₂ ³⁺	22.54	14.37	809	0.88
Cr(phen)(CN) ₄ ⁻	24.45	12.75	691	0.75
cis-Cr(bpy) ₂ (CN) ₂ ⁺	23.72	13.22	724	0.79
cis-Cr(phen) ₂ (NCS) ₂ ⁺	19.61	12.63	712	0.78
cis-Cr(bpy) ₂ (NCS) ₂ ⁺	19.80	12.65	712	0.78

^a 10Dq of the Cr^{III}(PP)_nX_{6-2n} complexes calculated on the basis of that of their parent complexes by using the weighted average. ^b For ²E → ⁴A₂ transition. ^c B_{free} = 918 cm⁻¹ was used for gaseous Cr³⁺ from ref 32. ^d Reference 57. ^e References 2d and 32. ^f Reference 20. ^g References 19 and 20.

sum of the temperature-independent radiative (k_r) and nonradiative relaxation rate (k_{nr}⁰) constants and k(T) is the temperature-dependent nonradiative relaxation rate constant.

For all complexes considered here, plots of ln k against T⁻¹ display two distinct regions as illustrated in Figure 6. The temperature-independent lifetime, [k(TI)]⁻¹ (set equal to the 77 K lifetime), activation energy, E_a, and a corresponding preexponential factor, A, from the thermally activated regions of the curves in Figure 6 are collected in Table VI.

The apparent thermal activation energies (32.9 ± 2 kJ mol⁻¹) and the preexponential factors ((3.5 ± 1.1) × 10¹¹ s⁻¹) are very similar for most of the mixed (polypyridyl)chromium(III) complexes. The cyano(polypyridyl)chromium(III) complexes differ only in that they have larger preexponential factors (by a factor of 20).

The Cr(phen)(CN)₄⁻ complex showed two different thermally activated regions from +25 to -28 °C and from -41 to -100 °C. Cr(PP)₂(NCS)₂⁺ complexes have longer lifetimes in DMF/CHCl₃ (3:1 v/v) than in DMSO/H₂O (1:1 v/v) at 77 K (Table VI). Ambient-temperature lifetimes were not sensitive to the presence of oxygen.

(25) Endicott, J. F.; Lessard, R. B.; Lei, Y.; Ryu, C. K.; Tamilarasan, R. In *Excited States and Intermediates*; Lever, A. B. P., Ed.; ACS Symposium Series 307; American Chemical Society: Washington, D.C., 1986; p 85.

Table VIII. Absorption Maxima of Cr^{III}(bpy)_nX_{6-2n}

complex	10 ⁻³ λ _{max} , cm ⁻¹ (ε, M ⁻¹ cm ⁻¹)			
	broad bands	narrow bands		
Cr(bpy) ₃ ³⁺ ^a		22.00 (260)	23.40 (610)	25.10 (900)
Cr(bpy) ₂ Cl ₂ ^b	18.08 (43.7)	22.47 (90, sh)	23.92 (210)	25.32 (270)
Cr(bpy) ₂ (H ₂ O) ₂ ³⁺ ^b	20.31 (44.8)	22.32 (94.2)		
Cr(bpy) ₂ (NH ₃) ₂ ³⁺ ^c		22.22 (≈121)	23.81	25.32
Cr(bpy) ₂ (CN) ₂ ^d		22.22 (156, sh)	23.81 (362, sh)	25.32 (519, sh)
Cr(bpy)(NH ₃) ₄ ³⁺ ^c	21.48 (41, sh)	22.47 (59)	24.10 (84)	25.64 (119)
Cr(bpy)(en) ₂ ³⁺	21.51 (78, sh)	22.32 (104)	23.92 (124)	25.64 (163)
Cr(bpy) ₂ (NCS) ₂ ^d	19.80 (134)			
Cr(bpy) ₂ (ox) ^d	19.61 (60)	22.37 (90, sh)	23.98 (220, sh)	25.51 (364, sh)
average		22.30 ± 0.15	23.85 ± 0.22	25.41 ± 0.22

^a Reference 19. ^b Reference 14 and this work. ^c Reference 15. ^d Reference 30.

Values of $10Dq$ can be estimated by using the approach of König and Herzog¹⁹ consistent with the variations of the observed doublet excited-state energies (Table VII) and by using the Stokes shift of Cr(NH₃)₆³⁺.²⁶ Expressions derived from the matrices of Tanabe and Sugano²⁷ using second-order perturbation theory assuming $C = 4B^{28}$ may be applied to the energies of the spin-forbidden transitions. The resulting values of $10Dq$, the Racah parameter B_{55} , and the nephelauxetic ratios β_{55} are listed in Table VII. The mixed (polypyridyl)chromium(III) complexes have smaller nephelauxetic ratios, β_{55} , than found for Cr(NH₃)₆³⁺ and Cr(en)₃³⁺ complexes; the values found for the cyano(polypyridyl)- and (thiocyanato)(polypyridyl)chromium(III) complexes are smaller than those found for Cr(PP)₃³⁺ and show greater covalency than the (am(m)ine)(polypyridyl)chromium(III) complexes.

Discussion

The study of electronic excited states must necessarily be concerned with their creation as well as their chemical behavior and their decay characteristics. Long-lived excited states are rarely populated efficiently by direct excitation. Rather, high-energy spin-allowed excited states are initially generated by light absorption, and the long-lived states of interest are populated by means of a cascade through intermediate excited states that have a variety of electronic configurations. These intermediate states sometimes have decay pathways that do not involve population of the lowest energy state of interest (thus affecting the efficiency, η_D , of its population), and some of these states, especially in transition-metal complexes, may be close enough in energy to the lowest energy excited state to affect its decay and reaction behavior. For these reasons, we have examined the ground-state absorption spectra of the Cr^{III}(PP)_nX_{6-2n} complexes as well as their ²E excited-state behavior.

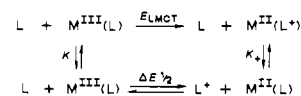
A. Ground-State Absorption Spectra. The ligand field absorption spectra of octahedral Cr(III) complexes typically consist of three spin-allowed (⁴A_{2g} → ⁴T_{ng}; $n = 1, 2$) transitions. These can only be observed if ligand absorbances do not interfere. Unfortunately, the polypyridyl ligands contribute to the absorption in the ligand field absorption region. Assuming octahedral microsymmetry for Cr(bpy)₃³⁺ and deconvoluting the absorption envelope into Gaussian components, König and Herzog¹⁹ assigned the three spin-allowed quartet bands at 23.4×10^3 , 28.9×10^3 , and 35.5×10^3 cm⁻¹ (centers of gravity of band maxima) to the transitions of ⁴A₂ → ⁴T₂, ⁴A₂ → ⁴T₁(F), and ⁴A₂ → ⁴T₁(P), respectively. Ligand-centered absorptions were assigned at 32.7×10^3 and 42.1×10^3 cm⁻¹. Three shoulders centered at 23.4×10^3 cm⁻¹ were assigned to vibrational components of the ⁴A₂ → ⁴T₂ transition. Serpone et al.²⁰ have concurred in this assignment, whereas Schläfer and co-workers²⁹ have based their ligand field splitting parameter, $\Delta = 22.0 \times 10^3$ cm⁻¹ for Cr(bpy)₃³⁺, on assignment of the lowest energy component of this collection of absorption bands to the ⁴A₂ → ⁴T₂ transition. Finally, Josephsen

and Schäffer¹⁴ have suggested that $\Delta = E(^4T_2) = 21.44 \times 10^3$ and 21.4×10^3 cm⁻¹, respectively, for Cr(bpy)₃³⁺ and Cr(phen)₃³⁺. This last assignment results in increasing values of Δ for phen < bpy < NH₃ < en, according to the average environment rule.

This confusion is a consequence of the steep rises in absorption toward the ultraviolet region that make assignment of the ligand field absorption maxima and their absorptivities difficult in Cr(PP)₃³⁺,^{19,20,29} and the mixed (polypyridyl)chromium(III) complexes.^{14,15,30} These mixed (polypyridyl)chromium(III) complexes have C₂ or C_{2v} symmetry. Consequently, the bands of cubic parentage, ⁴A_{2g} → ⁴T_{2g} (O_h), should split into three components, but the extent of this splitting is often too small to be resolved in solution spectra³¹ at ambient temperature. Moreover, the relatively narrow spectroscopic components observed for the Cr^{III}(PP)_nX_{6-2n} complexes have not been observed in other D_{3d} (e.g., Cr(en)₃³⁺,³¹ Cr(acac)₃,³² and Cr(TACN)₂³⁺³³) or lower symmetry complexes with saturated ligands. As a consequence, these bands have sometimes been assigned^{19,20} to vibrational transitions within the polypyridyl ligand. This assignment implies a significant amount of electron delocalization (or charge-transfer character) associated with these transitions.

We have been surprised to find that all mixed (bipyridyl)chromium(III) complexes exhibit the same three narrow bands. Their energies are at $(22.30 \pm 0.15) \times 10^3$, $(23.85 \pm 0.22) \times 10^3$, and $(25.41 \pm 0.2) \times 10^3$ cm⁻¹, respectively, independent of X (Table VIII). The energy differences between the individual components are about 1550 cm⁻¹, which does approximately correspond to some vibrational stretching bands of the bipyridyl ring.¹⁹ However, the energies of these bands are insensitive to the substitution of X ligands into the Cr(III) coordination sphere, while $E_{1/2}$ (Cr^{III}/Cr^{II}) is sensitive to such substitutions (Table IV). Since the energy required to populate the CT state is a strong first-order function of $E_{1/2}$ (Cr^{III}/Cr^{II}),³⁴⁻³⁶ this rules out any

- (29) Schläfer, H. L.; Gausmann, H.; Witzke, H. J. *J. Chem. Phys.* **1967**, *46*, 1423.
 (30) Broomhead, J. A.; Dwyer, M.; Kane-Maguire, N. *Inorg. Chem.* **1968**, *7*, 1388.
 (31) Perumareddi, J. R. *Coord. Chem. Rev.* **1969**, *4*, 73.
 (32) Lever, A. B. P. *Inorganic Electronic Spectroscopy*, 2nd ed.; Elsevier: Amsterdam, The Netherlands, 1984.
 (33) Wiegardt, K.; Schmidt, W.; Herrmann, W.; Küppers, H. *J. Inorg. Chem.* **1983**, *22*, 2953. TACN = 1,4,7-triazacyclononane.
 (34) The relationship between the energies of LMCT (or MLCT) transitions and the reduction potentials of the metal center has been developed in a number of places.^{35,36} For the present discussion it is sufficient to consider the simple cycle (where M is the coordination complex fragment, L is the polypyridyl ligand)



where $\Delta E_{1/2} = -E_{1/2}(L^+/L) + E_{1/2}(M^{III}/M^{II})$ and $E_{LMCT} = RT \ln K_+ + E_{1/2}(M^{III}/M^{II}) - E_{1/2}(L^+/L)$. Since K_+ and $E_{1/2}(L^+/L)$ are not strong functions of M, E_{LMCT} will vary as $E_{1/2}(M^{III}/M^{II})$, for any specific ligand L.

- (35) Cannon, R. D. *Adv. Inorg. Chem. Radiochem.* **1979**, *21*, 179.

(26) Wilson, R. B.; Solomon, E. I. *Inorg. Chem.* **1978**, *17*, 1729.

(27) (a) Tanabe, Y.; Sugano, S. *J. Phys. Soc. Jpn.* **1954**, *9*, 753. (b) *Ibid.* **1954**, *9*, 766.

(28) Jørgensen, C. K. *Adv. Chem. Phys.* **1963**, *5*, 33.

Table IX. Pseudotetragonal Ligand Field Parameters of Cr^{III}(PP)_nX_{6-2n}^a

complex	10Dq × 10 ⁻³ , cm ⁻¹	Dt, ^b cm ⁻¹	Ds, ^c cm ⁻¹	Δt ₂ , ^d cm ⁻¹	α ^e	n(xy) ^f	$\bar{n}(\epsilon_g)$ ^g
Cr(phen) ₂ (NH ₃) ₂ ³⁺	22.60	49	3	-236	-0.029	0.93	1.03
Cr(phen)(en) ₂ ³⁺	22.73	-42	11	243	0.035	1.07	0.96
Cr(bpy)(en) ₂ ³⁺	22.54	-39	17	246	0.035	1.07	0.96
Cr(bpy) ₂ (CN) ₂ ⁺	23.72	-90	-147	9	0	1	1
Cr(phen)(CN) ₄ ⁻	24.45	87	141	-12	0	1	1
Cr(phen) ₂ (NCS) ₂ ⁺	19.61	159	167	-621	-0.088	0.83	1.09
Cr(bpy) ₂ (NCS) ₂ ⁺	19.80	155	161	-616	-0.087	0.83	1.09
Cr(bpy) ₃ ³⁺	23.24			750 ^h	-0.13	0.74	1.13
Cr(phen) ₃ ³⁺	23.36			750 ^h	-0.13	0.74	1.13

^a Sign convention of ref 31 was followed. ^b Dt = -(2/7)(Dq_z - Dq_L) for *cis*-CrL₄Z₂ in ref 32. ^c Ds = -(1/7)(σ_z - σ_L + π_z - π_L) for *cis*-CrL₄Z₂ in ref 32; data for σ_i and π_i from ref 5a and this work. ^d Opposite sign compared to that in ref 50 for *cis* complexes, not including Cr(PP)₃³⁺. ^e Tetragonal mixing coefficient α = Δt₂/|D/2 + [D²/4 + (Δt₂)²]^{1/2} for Cr^{III}(PP)_nX_{6-2n} and trigonal mixing coefficient β = Δτ₂/D/2 + [D²/4 + (Δτ₂)²]^{1/2} for Cr(PP)₃³⁺ from ref 50; the energy gap between ²T₁ and ²T₂, D = 7000 and 5500 cm⁻¹ for Cr^{III}(PP)_nX_{6-2n} and Cr(PP)₃³⁺, respectively. ^f Orbital occupation number (OON) of the d_{xy} orbital, n(xy) = 1 + 2α/(1 + α²) for Cr^{III}(PP)_nX_{6-2n}, assuming ²T₁ emitting state, and OON of the "a" orbital, n(a) = 1 + 2β/(1 + β²) for Cr(PP)₃³⁺. ^g Average OON of (d_{xz}, d_{yz}) orbitals, $\bar{n}(\epsilon_g) = 1 - \alpha/(1 + \alpha^2)$ for Cr^{III}(PP)_nX_{6-2n} and average OON of the "e" orbital, $\bar{n}(\epsilon) = 1 - \beta/(1 + \beta^2)$ for Cr(PP)₃³⁺. ^h From trigonal splitting, Δτ₂; see text.

significant charge-transfer component of these transitions. It has been reported that Zn(bpy)₃²⁺ and Rh(bpy)₃³⁺ complexes exhibit only the perturbed ligand-centered transitions; Co^{III}(bpy)_nX_{6-2n} (X = NH₃, Cl⁻, H₂O, OH⁻; n = 1-3)^{14,15} complexes also exhibit the ligand-centered band but with a rather well-isolated d-d band. Thus, the Cr^{III}(PP)_nX_{6-2n} complexes are unique in exhibiting three common, relatively narrow bands. Gondo³⁹ has investigated the electronic structure and the spectrum of the free *cis*-2,2'-bipyridyl ligand. According to his calculation, there are three spin-allowed transitions, labeled by him ¹A₁(1) → ¹B₁(1), ¹B₁(2), and ¹B₁(3), which should appear at about 37.0 × 10³, 43.3 × 10³, and 50.5 × 10³ cm⁻¹, respectively. The two lower energy bands are in reasonable agreement with König and Herzog's assignment, with a red shift upon coordination of the ligand.^{19,37,39,40} Four spin-forbidden transitions, i.e. ¹A₁(1) → ³B₁(1), ³B₁(2), ³B₁(3), and ³B₁(4), were also considered, and these were estimated to have maxima at 30.9 × 10³, 32.8 × 10³, 34.5 × 10³, and 43.5 × 10³ cm⁻¹, respectively. It is interesting to note that the spacings between the first three spin-forbidden bands are 1900 and 1700 cm⁻¹, respectively. The highest energy band would be obscured by a spin-allowed transition. Ohno et al.⁴⁰ have suggested that a paramagnetic metal ion such as Cr³⁺ enhances the triplet, ligand-centered transitions of an aromatic compound on coordination. The mechanism for this enhancement of the transition moment is spin-spin coupling, mediated by the exchange interaction, between the (⁴A₂)Cr(III) center and the triplet states of the aromatic ligand. This coupling gives rise to molecular excited states of net spin multiplicities of 4 and 2 (assuming D₃ symmetry). To the extent that spin-spin coupling is important, the ⁴(⁴A₂, ¹L) → ⁴(⁴A₂, ³L) transition is spin allowed.

In view of these considerations we assign the transitions observed at (22.30 ± 0.15) × 10³, (23.85 ± 0.22) × 10³, and (25.41 ± 0.2) × 10³ cm⁻¹ in the Cr^{III}(PP)_nX_{6-2n} complexes to ⁴(⁴A₂, ¹A₁(1)) → ⁴(⁴A₂, ³B₁(1)), ⁴(⁴A₂, ³B₁(2)), and ⁴(⁴A₂, ³B₁(3)) transitions, respectively. This assignment is supported by the reasonable agreement between the observed (1550 cm⁻¹) and calculated (1800 cm⁻¹) spacings of these transitions.

While the exact assignments of the d-d band maxima remain elusive owing to competing absorbances, Hauser et al.⁴¹ have recently used the single-crystal polarized absorption spectra of Cr(bpy)₃(PF₆)₃ and the polarized absorption and emission spectra

of [Rh(bpy)₃](PF₆)₃/Cr³⁺ (dilute in Cr³⁺) at 1.4 and 10 K to identify the origin of the lower component for the transition ⁴A₂ → ⁴T₂ at 19 999 cm⁻¹. This transition has vibronic sidebands corresponding to vibrational frequencies of 164, 372, and 665 cm⁻¹, similar to those observed in the emission spectrum.

B. Emission Spectra. Although the interpretation of absorption spectra of the Cr^{III}(PP)_nX_{6-2n} complexes has been controversial,^{15,19,20,42} the origins of emission spectra are known to be pure ligand field transitions (²E, ²T₁ → ⁴A₂).^{19,20,42-44} McCathy and Vala⁴⁵ determined the single-crystal polarized electronic absorption and emission spectra of Cr(en)₃Cl₃·KCl·6H₂O, verified by Flint and Matthews⁴⁶ with bands at 14 883 and 14 901 cm⁻¹ assigned to ²E → ⁴A₂ transitions and the bands at 15 427, 15 439, and 15 517 cm⁻¹ assigned as the components of ²T₁ → ⁴A₂ transition. From a detailed examination of the absorption and emission spectra of a single crystal of Rh(bpy)₃(PF₆)₃/Cr³⁺, Hauser et al.⁴¹ confirmed König and Herzog's assignments¹⁹ of the ²E → ⁴A₂ transition at 13 750 cm⁻¹ with 19.5-cm⁻¹ splitting and the ²T₁ → ⁴A₂ transitions at 14 350 and 14 438 cm⁻¹. Thus, very similar splittings are reported for the ²E (18 and 19.5 cm⁻¹) and the ²T₁ (80 and 88 cm⁻¹) states of Cr(en)₃³⁺ and Cr(bpy)₃³⁺, respectively. Hoggard⁴⁷ has recently estimated the energy difference between the ²E and ²T₁ bands of Cr(en)₃³⁺ using the full configuration interaction and the known ligand angular geometry (defined by the Cartesian bite angle α and the Cartesian twist angle β). He predicted that one component of the ²T₁ set would move toward the ²E set with increasing bite or twist angle. For a 90° bite angle he calculated the energy difference between these components to be about 600 cm⁻¹. The observed values are about 540 cm⁻¹ for Cr(en)₃³⁺,^{46,47} 700 cm⁻¹ for Cr(bpy)₃³⁺,^{19,20,42,44} and 600 cm⁻¹ for Cr(phen)₃³⁺.²⁰

The ligand field strength exerted by two of 1,4,7-triazaacyclononane (TACN) ligands in a bis complex has been postulated to be the same as that exerted by phenanthroline and bipyridine ligands in their tris complexes.⁴⁸ Thus, we assume that 10Dq of Cr(PP)₃³⁺ complexes is approximately equal to that of Cr(TACN)₂³⁺ complexes. The energy of the spin-forbidden transition ²E ↔ ⁴A_{2g} in Cr(III) complexes (O_h) depends on the interelectron repulsion integrals, which for ΔE = E(²E_g) - E(⁴A_{2g}) are given in eq 4,³² where spin-orbit coupling has been neglected.

$$\Delta E = 9B + 3C - 90B^2/10Dq \quad (4)$$

- (36) (a) Endicott, J. F.; Ferraudi, G. J.; Barber, J. R. *J. Phys. Chem.* **1975**, *79*, 630. (b) Endicott, J. F. *Inorg. Chem.* **1977**, *16*, 494. (c) Endicott, J. F. In *Concepts of Inorganic Photochemistry*; Adamson, A. W., Fleischauer, P. D., Eds.; Wiley: New York, 1975; Chapter 3, p 81.
 (37) Ohno, T.; Kato, S. *Bull. Chem. Soc. Jpn.* **1974**, *47*, 2953.
 (38) Maestri, M.; Sandrini, D.; Balzani, V.; Maeder, U.; von Zelewsky, A. *Inorg. Chem.* **1987**, *26*, 1323.
 (39) Gondo, Y. *J. Chem. Phys.* **1964**, *41*, 3928.
 (40) Ohno, T.; Kato, S.; Kaizaki, S.; Hanzaki, I. *Chem. Phys. Lett.* **1983**, *02*, 471.
 (41) Hauser, A.; Mäder, M.; Robinson, W. T.; Murugesan, R.; Ferguson, J. *Inorg. Chem.* **1987**, *26*, 1331.

- (42) Ferguson, J.; Herren, H.; Krausz, E. R.; Maeder, M.; Vrbancich, J. *Coord. Chem. Rev.* **1985**, *64*, 21.
 (43) Serpone, N.; Hoffman, M. Z. *J. Phys. Chem.* **1987**, *91*, 1737.
 (44) Henry, M. S.; Hoffman, M. Z. *Inorganic and Organometallic Photochemistry*; Wrighton, M. S., Ed.; Advances in Chemistry 168; American Chemical Society: Washington, D.C., 1978; p 91.
 (45) McCathy, P. J.; Vala, M. T. *Mol. Phys.* **1973**, *25*, 17.
 (46) Flint, C. D.; Matthews, A. P. *J. Chem. Soc., Faraday Trans. 2* **1976**, *72*, 579.
 (47) Hoggard, P. E. *Coord. Chem. Rev.* **1986**, *70*, 85.
 (48) Boeyens, J. C. A.; Forbes, A. G. S.; Hancock, R. D.; Wiegardt, K. *Inorg. Chem.* **1985**, *24*, 2926.

One would expect that the energies of the 2E excited states are similar to each other for the Cr(III) complexes in which the $\text{Cr}^{\text{III}}\text{N}_6$ chromophore has same molecular symmetry (D_{3d}) and similar values of $10Dq$. However, the energies of the 2E excited states of $\text{Cr}(\text{PP})_3^{3+}$ ($13.74 \times 10^3 \text{ cm}^{-1}$)²⁰ complexes differ from those of $\text{Cr}(\text{TACN})_2^{3+}$ ($14.72 \times 10^3 \text{ cm}^{-1}$)^{2d} by 980 cm^{-1} . This difference arises from the perturbation of the 2E excited state mainly due to the π character of the polypyridyl ligand.^{49,50} In view of this, we have assumed that the differences in $E({}^2E)$ between $\text{Cr}(\text{PP})_3^{3+}$ and $\text{Cr}(\text{TACN})_2^{3+}$ complexes are approximately proportional to the π -interaction energy of the polypyridyl ligands in $\text{Cr}(\text{PP})_3^{3+}$ complexes. Thus, we obtain $\pi_{\text{bpy}} \cong \pi_{\text{phen}} \cong -250 \text{ cm}^{-1}$, $\sigma_{\text{bpy}} \cong 7.41 \times 10^3 \text{ cm}^{-1}$, and $\sigma_{\text{phen}} \cong 7.45 \times 10^3 \text{ cm}^{-1}$ for $\text{Cr}(\text{bpy})_3^{3+}$ and $\text{Cr}(\text{phen})_3^{3+}$, respectively, from the equality $10Dq = 3\sigma_L - 4\pi_L$ using $10Dq$ values in Table IX for $\text{Cr}(\text{PP})_3^{3+}$. σ_L of Cr/TACN is equal to $7.59 \times 10^3 \text{ cm}^{-1}$ (i.e. $10Dq/3$; the value of the π_L parameter of a saturated amine or an ammine is usually set to 0).^{5,47} The Dt ,³¹ Ds ,³² and Δt_2 ⁵⁰⁻⁵² values for $\text{Cr}^{\text{III}}(\text{PP})_n\text{X}_{6-2n}$ complexes (all C_{2v} symmetry) based on these parameters are collected in Table IX. The tetragonal parameter Δt_2 has been used to calculate the splitting patterns of the doublet excited states (2E_g , ${}^2T_{1g}$ in O_h).⁵⁰⁻⁵² Most of the cis complexes examined to date seem to be 2E emitters due to the smaller tetragonal splitting as compared to that of the trans complexes. It has also been suggested that the states of 2E_g and ${}^2T_{1g}$ parentage cross at $|\Delta t_2| \cong 2000 \text{ cm}^{-1}$, except that *trans*- $\text{Cr}(\text{en})_2(\text{H}_2\text{O})_2^{3+}$ is a 3E emitter even though $\Delta t_2 = 2200 \text{ cm}^{-1}$.^{52a} Ceulemans et al.⁵⁰ showed that when $0 \leq \Delta t_2 \leq 2000 \text{ cm}^{-1}$, a low-energy component of the 2T_1 states approaches the value of $E({}^2E)$. As shown in Table IX, all mixed (polypyridyl)chromium(III) complexes have $|\Delta t_2| \leq 250 \text{ cm}^{-1}$ except $\text{Cr}(\text{PP})_2(\text{NCS})_2^+$ ($\sim 620 \text{ cm}^{-1}$). Therefore, one would expect the energy gaps between 2E and a low-energy component of 2T_1 states to be smaller than those of the parent complexes. Upon substitution of one or two polypyridyls by NH_3 , CN^- , or en, this energy gap between the 2E excited state and the lower component of the 2T_1 excited state is indeed reduced to 150–270 cm^{-1} (Table V).

In the D_{3d} parent complexes, the trigonal splitting⁵⁰ has been defined as

$$\Delta\tau_2 = 3\pi_{\perp}(\psi) - 3\pi_{\perp}(\chi) \quad (5)$$

where $\pi_{\perp}(\psi)$ and $\pi_{\perp}(\chi)$ are in phase and out of phase combinations of ligand π orbitals, respectively. It is useful to consider the following relationships between the splitting parameters for tetragonal and trigonal symmetries:

$$|\Delta t_2(C_{2v})| \cong |\Delta t_2(C_{4v})| \cong \frac{1}{2}|\Delta t_2(D_{4h})| \cong \frac{1}{3}|\Delta\tau_2(D_{3d})| \quad (6)$$

The relationships within tetragonal symmetries are well-known,³² and the relationship between tetragonal and trigonal systems is also valid as long as eq 5 is valid for unsaturated ligands. Ceulemans et al.⁵⁰ qualitatively show that in tetragonal symmetry (C_{2v}) one of the 2T_1 components approaches and crosses the 2E state as Δt_2 varies, while the energy of the 2E excited state remains constant. In trigonal symmetry (D_{3d}) the energy of the 2E excited state changes, in the same manner as does that of the 2T_1 excited state in tetragonal symmetry, as $\Delta\tau_2$ varies while the energy of the 2T_1 excited state remains almost constant with some splittings.⁵⁰ This implies that the energy of the 2T_1 state in C_{2v} symmetry and of the 2E state in D_{3d} symmetry is very sensitive to the π character of the coordination sphere. As shown in Figure 7, on going from $\text{Cr}(\text{en})_3^{3+}$ to $\text{Cr}(\text{PP})_3^{3+}$ complexes, the energy of the 2T_1 component is initially decreased and then becomes more or less con-

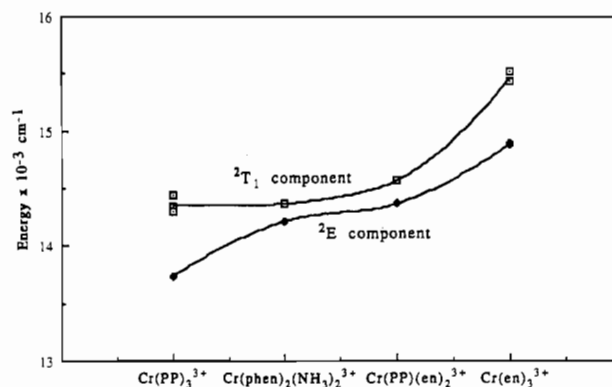


Figure 7. Variations in doublet-excited-state electronic origins of $\text{Cr}^{\text{III}}(\text{PP})_n\text{X}_{6-2n}$ with ligand permutations.

stant while the energy of the 2E set decreases continuously. These observations are consistent with predictions from the tetragonal splitting parameters (Table IX). The energies of the 2T_1 components for $\text{Cr}(\text{phen})_2(\text{NH}_3)_2^{3+}$, $\text{Cr}(\text{phen})(\text{en})_2^{3+}$, and $\text{Cr}(\text{bpy})(\text{en})_2^{3+}$ should be almost the same because they have very similar values of $|\Delta t_2| = 242 \pm 5 \text{ cm}^{-1}$. From eq 6, $\text{Cr}(\text{PP})_3^{3+}$ complexes also have values of $|\Delta\tau_2|$ comparable with those of tetragonal complexes. Thus, the 2E excited-state energies of $\text{Cr}(\text{phen})_2(\text{NH}_3)_2^{3+}$ and $\text{Cr}(\text{PP})(\text{en})_2^{3+}$ are similar to one another because they have similar AOM parameters^{5a} (σ_i and π_i in Table IX), but they are lower than those of $\text{Cr}(\text{NH}_3)_6^{3+}$ and $\text{Cr}(\text{en})_3^{3+}$ (σ -donor ligands) and higher than $E[({}^2E)\text{Cr}(\text{PP})_3^{3+}]$ (good σ -donor as well as π -acceptor ligands). Therefore, the energy gap between the 2E excited state, which is not dependent on $|\Delta t_2|$, and one of the 2T_1 excited-state components, which is sensitive to $|\Delta t_2|$, should be smaller than that of their parent complexes as observed (Table V and Figure 7). The tetragonal (α) and trigonal (β) mixing coefficients are included in Table IX, along with the orbital occupation numbers, $n(i)$, of the t_{2g} orbitals in the Cr^{3+} complexes. The orbital occupation numbers (OON) for the 2T_1 emitting state in $\text{Cr}^{\text{III}}(\text{PP})_n\text{X}_{6-2n}$, $n(xy)$ and $\bar{n}(e_g)$, are close to unity, which strongly implies that all $\text{Cr}^{\text{III}}(\text{PP})_n\text{X}_{6-2n}$ are 2E emitters, which have one electron per t_{2g} orbital.⁵⁰ The higher energy electronic origin is most plausibly assigned as a low-energy component of the 2T_1 states, in agreement with calculations by several authors indicating that 2E splittings must be very small.^{23,47,53,54}

Substitution of polypyridyl by CN^- or NCS^- markedly reduced the energy separation of the 2E excited state and the 4A_2 ground state (Table IV). Since the nephelauxetic ratios of the cyanide and thiocyanate ligands are similar to⁴⁹ or smaller than those of NH_3 and en, comparable effects would be expected in $\text{Cr}(\text{bpy})_2(\text{CN})_2^+$ and $\text{Cr}(\text{PP})_2(\text{NCS})_2^+$ complexes (based on variations of B). As a consequence, the 2E - 4T_2 energy separation in $\text{Cr}(\text{PP})_2(\text{NCS})_2^+$ complexes is still large due to the strong ligand field of the polypyridyl ligand. This results in smaller 2E - 4A_2 energy separations in the $\text{Cr}(\text{PP})_2(\text{NCS})_2^+$ complexes than in the $\text{Cr}(\text{NCS})_6^{3-}$ parent.

The spectroscopic assignments have been incorporated into the qualitative energy level scheme shown in Figure 8.

C. Photophysics. The lifetimes, $\tau({}^2E)$, of the lowest energy, vibrationally equilibrated doublet excited states of Cr(III) complexes are generally strong functions of temperature. The detailed temperature dependencies vary from complex to complex and from solvent to solvent.^{2d,11} For purposes of the present discussion, it is useful to fit the observed temperature dependencies to eq 1–3.

At low temperatures $\tau({}^2E)$ approaches a well-defined limiting value, $[k(\text{TI})]^{-1}$, which is usually independent of the condensed-phase matrix. The 2E lifetime is strongly temperature dependent in fluid solutions at ambient temperatures. The transition between

(49) (a) Flint, C. D.; Greenough, P. J. *Chem. Soc., Faraday Trans. 2* **1974**, *70*, 815. (b) Flint, C. D.; Matthews, A. P. *J. Chem. Soc., Faraday Trans. 2* **1974**, *70*, 1301.

(50) Ceulemans, A.; Bongaerts, N.; Vanquickenborne, L. G. *Inorg. Chem.* **1987**, *26*, 1566.

(51) Flint, C. D.; Matthews, A. M.; O'Grady, P. J. *J. Chem. Soc., Faraday Trans. 2* **1977**, *73*, 655.

(52) (a) Forster, L. S.; Rund, J. V.; Fucaloro, A. F. *J. Phys. Chem.* **1984**, *88*, 5012. (b) Fucaloro, A. F.; Forster, L. S.; Glover, S. G.; Kirk, A. D. *Inorg. Chem.* **1985**, *24*, 4242.

(53) Geiser, U.; Güdel, H. U. *Inorg. Chem.* **1981**, *20*, 3013.

(54) Flint and Matthews²³ have claimed that the splitting of the 2E state by the tetragonal perturbation in $\text{Cr}(\text{NH}_3)_5\text{X}^{2+}$ ($\text{X} = \text{Cl}^-, \text{Br}^-, \text{I}^-, \text{ONO}_2^-, \text{ONO}^-, \text{CF}_3\text{COO}^-, \text{H}_2\text{O}$) is 100–300 cm^{-1} .

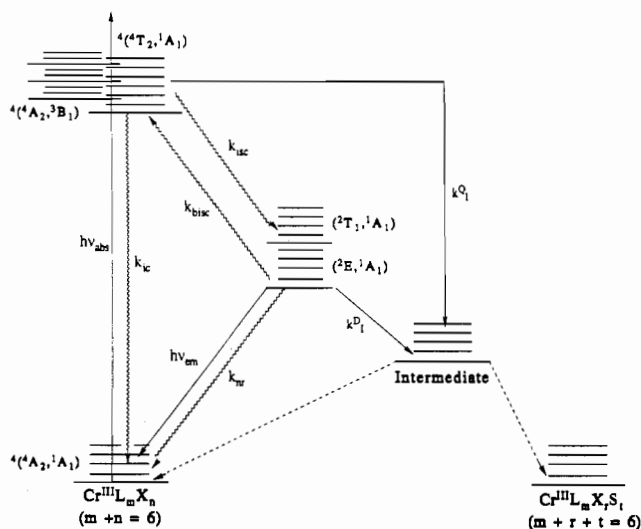


Figure 8. Qualitative energy level scheme for $\text{Cr}^{\text{III}}(\text{PP})_n\text{X}_{6-2n}$. The rate constants are for nonradiative relaxation (k_{nr}), intersystem crossing (k_{ISC}), back intersystem crossing (k_{BISC}), and photochemical reaction (k^{R}) in quartet ($\text{R} = \text{Q}$) and doublet ($\text{R} = \text{D}$) excited states. The intermediate is the substitutional intermediate species with solvent S. Approximate state designations in parentheses indicate the electronic states of the Cr^{III} center and a polypyridyl ligand, respectively. The external superscript designates the net spin multiplicity resulting from spin-spin coupling between the metal and ligand centers.

the thermally activated and the temperature-independent decay regions is at about 165 K for the $\text{Cr}^{\text{III}}(\text{PP})_n(\text{CN})_{6-2n}$ complexes and about 200 K for the other $\text{Cr}^{\text{III}}(\text{PP})_n\text{X}_{6-2n}$ complexes. Only for the cyano complexes does this transition range occur in the glassy matrix.

The excited-state lifetimes depend on the sum of radiative and nonradiative relaxation rates; i.e., $[\tau(^2\text{E})]^{-1} = k_r + k_{\text{nr}}$, where $k_{\text{nr}} = k_{\text{nr}}^0 + k(T)$, and k_r and k_{nr}^0 are nearly temperature independent. Values of k_{nr}^0 can be attributed to the probability of nuclear and electronic tunneling between the nested ^2E and $^4\text{A}_2$ potential energy surfaces. These tunneling probabilities are thought to depend on the energy gap, $E(^2\text{E}) - E(^4\text{A}_2)$, and the number of high-frequency acceptor vibrations (e.g., N-H stretching modes) coupled to the relaxation coordinate.⁵⁵⁻⁵⁷ These ideas are qualitatively consistent with the variations of $k(\text{TI})$ among the compounds considered here. A more detailed consideration of the low-temperature relaxation behavior of a wider variety of Cr^{III} complexes will be presented elsewhere.⁵⁸

We were disappointed to find that $(^2\text{E})\text{Cr}(\text{PP})_n\text{X}_{6-2n}$ complexes are much more short-lived at 298 K than their $(^2\text{E})\text{Cr}(\text{PP})_3^{3+}$ parents, in some instances by as much as a factor of 10^3 . The lifetimes of these complexes are all temperature dependent in the high-temperature regime. The nature of these thermally activated, nonradiative-decay pathways has been a major problem in Cr^{III} excited-state chemistry.² The pathways that have been suggested for thermally activated relaxation of $(^2\text{E})\text{Cr}(\text{III})^{2,25}$ have included back intersystem crossing to populate a reactive quartet excited state,^{2a,2c,59,60} chemical reaction within the doublet manifold,^{2e,61}

and crossing to the potential energy surface of a ground-state reaction intermediate.^{2d,7,9,24,25,44,62}

We have estimated the energy gap, $\Delta E(^4\text{T}_2 \rightarrow ^2\text{E}^0)$, and compared it with the measured activation energy (Table VI). These estimates are based on the $^4\text{T}_2$ band origins of $19.96 \times 10^3 \text{ cm}^{-1}$ for $\text{Cr}(\text{NH}_3)_6^{3+26}$ and $20.00 \times 10^3 \text{ cm}^{-1}$ for $\text{Cr}(\text{bpy})_3^{3+,41}$ and we used the method of Perumareddi³¹ for *cis*- $\text{Cr}^{\text{III}}\text{L}_4\text{X}_2$ complexes to estimate the variations in $E(^4\text{T}_2)$ when X is substituted for PP to form $\text{Cr}^{\text{III}}(\text{PP})_n\text{X}_{6-2n}$ complexes. The lowest spectroscopic transition was assumed to be to the $^4\text{B}_2(^4\text{T}_{2g})$ state when $Dq_x > Dq_y$, but to the $^4\text{E}(^4\text{T}_{2g})$ state when $Dq_x < Dq_y$. Values of $\Delta E(^4\text{T}_2 \rightarrow ^2\text{E}^0)$ vary from about 65 to 113 kJ mol^{-1} (or $(5.5-9.5) \times 10^3 \text{ cm}^{-1}$) for these complexes, while E_a for thermally activated ^2E relaxation varies by only slightly more than 2 kJ mol^{-1} . There may be some tendency of the ambient lifetimes, τ_{298} , to decrease as $\Delta E(^4\text{T}_2 \rightarrow ^2\text{E}^0)$ increases. However, any such effect appears mostly in the preexponential factor (A) in eq 3. Even though the absolute values of $E(^4\text{T}_2)$ remain in doubt, the trends in these energies, as the X ligands are changed, are reasonably certain. Consequently, our observations on this family of complexes are not consistent with deactivation arising simply from the thermal population of a high-energy excited state, and $^2\text{E} \rightarrow ^4\text{T}_2$ back intersystem crossing cannot contribute significantly to k_{nr} for more than one or two of the complexes listed in Table VI.

The variations in k_{nr} can be usefully discussed in terms of thermally activated surface crossings.^{2d,25} In such an approach the temperature-independent variations in the crossing rate can be attributed to differences in either or both of the (a) selection rules for the surface crossing and (b) densities of initial (ρ_i) and final (ρ_f) states in the surface-crossing region. A large difference between ρ_i and ρ_f is expected when the crossing is from a bound initial state to a final state near or above the dissociation limit for some bond or normal mode. The nuclear coordinates that are activated on surface crossing need not be the ones involved in bond breaking. This is especially the case if the surface crossing also involves change of electronic configuration to form some sort of reaction intermediate in its electronic ground state.

A frequently discussed model for relaxation of polypyridyl- $(^2\text{E})\text{Cr}(\text{III})$ excited states involves the association of a solvent molecule with the largely empty $t_{2g}(\text{O}_h)$ orbital of the metal excited state.^{2e,44} These excited electronic configurations contribute to the $^2\text{T}_{1g}(\text{O}_h)$ excited state in O_h and tetragonal complexes and to the $^2\text{E}_g(\text{O}_h)$ components in trigonally distorted complexes. However, among the complexes considered in this report, $(^2\text{E})\text{Cr}(\text{phen})_3^{3+}$ and $(^2\text{E})\text{Cr}(\text{bpy})_3^{3+}$ have the longest lifetimes and also the most unequal orbital populations (see Table IX). Apparently, an unequal orbital population in the ^2E (or neighboring $^2\text{T}_1$) excited state is not itself sufficient to provide a facile channel for relaxation.

Our observations on $\text{Cr}^{\text{III}}(\text{PP})_n\text{X}_{6-2n}$ complexes are largely inconsistent with the BISC hypothesis and require nuclear rearrangements and a solvent-dependent surface crossing (probably to some chemically altered "intermediate" species) to account for the thermally activated relaxation of their ^2E excited states, and this feature is included in Figure 8. There is as yet no simple, but detailed, model that can account for all the observations. Studies, now in progress,⁶³ of complexes containing ligands whose steric constraints severely restrict some nuclear motions while promoting others, may lead to such a model. However, there is no reason to believe that a simple model will be useful for all complexes. Rather, we expect that different classes of complexes will be able to access different excited-state relaxation channels.

(55) (a) Englman, R.; Jortner, J. *Mol. Phys.* **1970**, *18*, 145. (b) Freed, K. F.; Jortner, J. *J. Chem. Phys.* **1970**, *52*, 6272.

(56) (a) Fucaloro, A. F.; Forster, L. S.; Fund, J. V.; Lin, S. H. *J. Phys. Chem.* **1983**, *87*, 1796. (b) *Ibid.* **1984**, *88*, 5020. (c) Forster, L. S.; Rund, J. V.; Castelli, F.; Adams, P. *J. Phys. Chem.* **1982**, *86*, 2395. (d) Forster, L. S.; Mønsted, O. *J. Phys. Chem.* **1986**, *90*, 5131.

(57) Kühn, K.; Wasgestian, F.; Kupka, H. *J. Phys. Chem.* **1981**, *85*, 665.

(58) Ryu, C. K.; Lessard, R. B.; Endicott, J. F., submitted for publication in *J. Phys. Chem.*

(59) (a) Shipley, N. J.; Linck, R. G. *J. Phys. Chem.* **1980**, *84*, 2490. (b) Cimolino, M.; Linck, R. G. *Inorg. Chem.* **1981**, *20*, 3499. (c) Kirk, A. D. *J. Phys. Chem.* **1981**, *85*, 3205. (d) Castelli, F.; Forster, L. S. *J. Phys. Chem.* **1977**, *81*, 403 and references therein. (e) Sandrini, D.; Gandolfi, M.; Moggi, L.; Balzani, V. *J. Am. Chem. Soc.* **1978**, *100*, 1463.

(60) Linck, N. J.; Berens, S. J.; Magde, D.; Linck, R. G. *J. Phys. Chem.* **1983**, *87*, 1733.

(61) (a) Gutierrez, A. R.; Adamson, A. W. *J. Phys. Chem.* **1978**, *82*, 902. (b) Kang, Y. S.; Castelli, F.; Forster, L. S. *J. Phys. Chem.* **1979**, *83*, 2368. (c) Forster, L. S.; Castelli, F. *J. Phys. Chem.* **1980**, *84*, 2492.

(62) (a) Endicott, J. F. *J. Chem. Educ.* **1983**, *60*, 824. (b) Kane-Maguire, N. A. P.; Wallace, K. C.; Miller, D. B. *Inorg. Chem.* **1985**, *24*, 597.

(63) Lessard, R. B.; Ryu, C. K.; Perkovic, M.; Endicott, J. F., work in progress.

(64) Kirk, A. D.; Frederick, L. A.; Wong, C. F. C. *Inorg. Chem.* **1979**, *18*, 1468.

There are very likely some complexes for which the BISC pathway dominates.

Note Added in Proof. Waltz and co-workers⁶⁵ have just reported the first direct evidence for the generation of a chemically active intermediate as the product of (²E)Cr(III) excited-state relaxation. These workers find that an aquated, apparently 7-coordinate complex with a lifetime longer

(65) Waltz, W. L.; Lee, S. H.; Friesen, D. A.; Lilie, J. *Inorg. Chem.* **1988**, 27, 1133.

than $\tau(^2E)$ is formed in the thermally activated relaxation of *cis*-(²E)-Cr([14]aneN₄)(NH₃)₂³⁺ under ambient conditions in water.

Registry No. *cis*-[Cr(phen)₂(NH₃)₂](ClO₄)₃, 65888-21-3; [Cr(phen)₂(acac)](ClO₄)₂, 114581-93-0; *cis*-[Cr(phen)₂(NCS)₂](SCN), 114594-78-4; [Cr(phen)(CN)₄][Cr(phen)₂(CN)₂], 114581-96-3; Na-[Cr(phen)(CN)₄], 114581-97-4; [Cr(phen)(en)₂](ClO₄)₃, 114581-99-6; *cis*-[Cr(bpy)₂(CN)₂](ClO₄)₃, 114582-01-3; *cis*-[Cr(bpy)₂(NCS)₂](SCN), 114582-02-4; [Cr(bpy)(en)₂](ClO₄)₃, 114582-04-6; *cis*-[Cr(phen)₂Cl₂]Cl, 31282-15-2; *cis*-[Cr(phen)₂(H₂O)₂](NO₃)₃, 49726-42-3; *cis*-[Cr(phen)₂(TFMS)₂]TFMS, 114582-06-8; *cis*-[Cr(bpy)₂Cl₂]Cl, 26154-79-0; *cis*-[Cr(bpy)₂(TFMS)₂]TFMS, 114582-08-0; Cr(bpy)₃³⁺, 15276-15-0.

Contribution from the Department of Chemistry,
College of the Holy Cross, Worcester, Massachusetts 01610

Kinetic and Spectroscopic Studies of Mo(CO)₂(PR₃)₂Br₂ Compounds

Richard S. Herrick,* Christopher H. Peters, and Ronald R. Duff, Jr.

Received November 19, 1987

Flash-photolysis and stopped-flow experiments are reported for a series of aryl-, alkyl-, and mixed aryl-alkylphosphine derivatives of Mo(CO)₃(PR₃)₂Br₂. The photochemically generated dicarbonyl transient rapidly recombines with carbon monoxide under a CO atmosphere to re-form the tricarbonyl via the rate law $R = k[\text{Mo}(\text{CO})_2(\text{PR}_3)_2\text{Br}_2][\text{CO}]$. Bimolecular rate constants between 2.5×10^3 and $7.3 \times 10^5 \text{ M}^{-1} \text{ s}^{-1}$ were measured in 1,2-dichloroethane. The natural logarithm of the rate constants for CO recombination fit a two-parameter free energy relationship based on the electronic and steric nature of the phosphines. Electron-donating and sterically bulky phosphines inhibit reaction. There is a pronounced solvent effect on the reactivity and the electronic spectrum of dicarbonyl compounds. Hexane as solvent accelerates the reaction while methanol essentially quenches it relative to 1,2-dichloroethane. Electronic spectral measurements show that λ_{max} for the HOMO-LUMO transition shifts from 570 nm in CH₂Cl₂ to 755 nm on Teflon (diffuse-reflectance spectrum). These observations are consistent with solvent interaction with the LUMO.

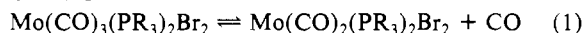
Introduction

The study of formally electron-deficient group 6 d⁴ complexes has recently enjoyed renewed interest in an effort to explain their counterintuitive stability. Among the systems that have been studied are the 6-coordinate compounds with the general formula M(CO)_n(RC≡CR)_{2-n}L₂X₂ (L₂X₂ = (PR₃)₂X₂, n = 1, 2;¹ L₂X₂ = (S₂CNR₂)₂, n = 0, 1, 2;² L₂X₂ = (π-C₅H₅)₂X, n = 0, 1;³ M = Mo, W; X = Cl, Br, I). Non-6-coordinate 16-electron d⁴ compounds have also been reported and generally have π-base alkyne ligands as in Mo(S-*t*-Bu)₂(CN-*t*-Bu)₂(RC≡CR).⁴ Crystallographic,⁵ spectroscopic,⁶ theoretical,^{5b,7} and electrochemical⁸ studies

have contributed greatly to an understanding of this stability now known to stem from the presence of both π-acid and π-base ligands or from severe distortion away from an ideal geometry.

Surprisingly, little mechanistic research has been reported for these compounds. A study of the reaction of alkynes with electron-deficient Mo(CO)(RC≡CR)(S₂CNR₂)₂ compounds⁹ demonstrated that substitution for carbon monoxide proceeds by a slow dissociative process while alkyne exchange proceeds by a faster associative step. The π-base alkyne ligand controls the reactivity by either stabilizing the 14-electron intermediate after CO loss or preferentially dissociating from the 18-electron intermediate following alkyne addition due to loss of the alkyne π-donor interaction in the saturated intermediate.

Kinetic studies have not been reported for systems containing no strongly π-donating ligand. We have initiated a mechanistic study of this class of electron-deficient compounds to explore their reactivity toward Lewis base nucleophiles. We chose to begin with a study of the addition of CO to Mo(CO)₂(PR₃)₂Br₂. This is a useful starting point because the compounds are isolable, have been amply characterized, contain simple monodentate ligands, and are in equilibrium with the corresponding 18-electron tricarbonyl¹⁰ (eq 1).



This paper gives the results of flash-photolysis studies of the tricarbonyl in the presence of excess carbon monoxide. Reaction rates of the photochemically generated dicarbonyl with carbon monoxide were determined by watching the disappearance of the d-d absorbance band of the dicarbonyl at around 600 nm.

- (1) (a) Anker, M. W.; Colton, R.; Tomkins, I. B. *Aust. J. Chem.* **1966**, 20, 9. (b) Moss, F. R.; Shaw, B. J. *J. Chem. Soc. A* **1970**, 595. (c) Winston, P. B.; Burgmayer, S. J. N.; Tonker, T. L.; Templeton, J. L. *Organometallics* **1986**, 5, 1707. (d) Davidson, J. L.; Vasapollo, G. J. *Chem. Soc., Dalton Trans.* **1985**, 2239.
- (2) (a) Templeton, J. L.; Ward, B. C. *Inorg. Chem.* **1980**, 19, 1753. (b) Ricard, L.; Weiss, R.; Newton, W. E.; Chen, G. J.-J.; McDonald, J. W. *J. Am. Chem. Soc.* **1978**, 100, 1318. (c) Herrick, R. S.; Templeton, J. L. *Organometallics* **1982**, 1, 842.
- (3) (a) Davidson, J. L.; Sharp, D. W. A. *J. Chem. Soc., Dalton Trans.* **1975**, 2531. (b) Davidson, J. L.; Green, M.; Stone, F. G. A.; Welch, A. J. *J. Chem. Soc., Dalton Trans.* **1977**, 287.
- (4) Kamata, M.; Yoshida, T.; Otsuka, S.; Hirotsu, K.; Higuchi, T.; Kido, M.; Tatsumi, K.; Hoffmann, R. *Organometallics* **1982**, 1, 227.
- (5) (a) Drew, M. G. B.; Tomkins, K. B.; Colton, R. *Aust. J. Chem.* **1970**, 23, 2517. (b) Cotton, F. A.; Meadows, J. H. *Inorg. Chem.* **1984**, 23, 4688.
- (6) (a) McDonald, J. W.; Newton, W. E.; Creedy, C. T. C.; Corbin, J. L. *J. Organomet. Chem.* **1975**, 92, C25. (b) Templeton, J. L.; Ward, B. C. *J. Am. Chem. Soc.* **1980**, 102, 3288.
- (7) (a) Kubacek, P.; Hoffmann, R. *J. Am. Chem. Soc.* **1981**, 103, 4320. (b) Templeton, J. L.; Winston, P. B.; Ward, B. C. *J. Am. Chem. Soc.* **1981**, 103, 7713.
- (8) Templeton, J. L.; Herrick, R. S.; Morrow, J. R. *Organometallics* **1984**, 3, 535.

(9) Herrick, R. S.; Leazer, D. M.; Templeton, J. L. *Organometallics* **1983**, 2, 834.

(10) Anker, M. W.; Colton, R.; Tomkins, I. B. *Rev. Pure Appl. Chem.* **1968**, 18, 23.